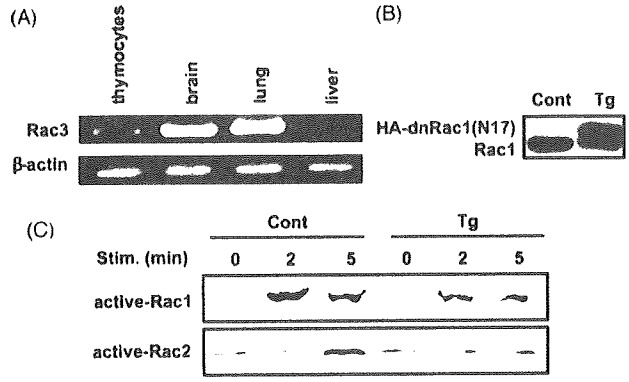

Fig. 1. TCR-induced activation of Rac1 and Rac2 was impaired in dnRac1-Tg mice. (A) RT-PCR analysis of Rac3 in the indicated tissues. (B) The expression of dnRac1N17 in total thymocytes isolated from dnRac1-Tg (Tg) and control (Cont) mice was detected by Western blotting with anti-Rac1. (C) Active Rac GTPases proteins were assayed by pull down with PBD beads from the lysates of total thymocytes with indicated stimulations and blotted with anti-Rac1 or Rac2 specific antibodies.

the proportion of CD4 CD8 double positive (DP) cells in the thymus was significantly decreased, while the proportion of double negative (DN) cells was increased (Fig. 2A and B). The ratio of DP to DN was strongly reduced, however, that of CD4-SP to DP was not changed, and the ratio of CD8-SP to DP was even slightly increased. For the calculation of the absolute number of mature CD8-SP in the thymus, we counted only TCRβ high cells in $CD8^+$ $CD4^-$ population to exclude immature CD8-SP. Absolute numbers of DN cells were normal in dnRac1-Tg mice and numbers of DP cells were decreased (Fig. 2C). From these results, transition from DN to DP, namely β-selection was significantly reduced in transgenic thymocytes. In transgenic mice, positive selection of CD4-SP was not affected, whereas positive selection of CD8-SP was slightly enhanced.

To confirm these results, we next investigated effects on positive selection using defined T cell receptor (TCR) specificity. We utilized class I restricted (OT-I) and class II restricted (OT-II) TCR transgenic mice, and crossed with dnRac1-Tg mice on a $RAG2^{-/-}$ background to avoid endogenous TCR rearrangement. As shown in Fig. 3, the ratios of DP to DN in both OT-I and OT-II were much less than controls, confirming impaired β-selection. In OT-II TCR Tg mice, the ratio of CD4-SP to DP is not reduced (Fig. 3B), indicating that positive selection of class II restricted TCR is not inhibited in the presence of dnRac1. In OT-I TCR Tg mice, the ratio of CD8-SP to DP was increased. This is consistent with the finding that generation of CD8-SP in the thymus is slightly increased by the inhibition of Rac GTPases.

3.2. Severe reduction of peripheral mature T cells in dnRac1-Tg mice

In thymi of dnRac1-Tg mice, we observed reduced numbers of CD4-SP T cells, but not of CD8-SP T cells (Fig. 2C), therefore, we next investigated subpopulations of peripheral mature T cells. As shown in Fig. 4, the proportion and absolute number of CD4-SP T cells in spleen of dnRac1-Tg mice were less than half of controls. The same magnitude of reduction was also observed in mesenteric lymph node (mLN) and peripheral blood (PBL). The reduction in the number of CD4-SP T cells in periphery was much severer than that observed in the thymus. Interestingly, the absolute numbers of CD8-SP T cells in spleen, mLN and PBL were also reduced in dnRac1-Tg mice (Fig. 4). In the thymi of dnRac1-Tg mice, the number of CD8-SP T cells was not reduced, therefore a reduction in the number of mature T cells in periphery cannot solely be attributed to the impaired generation of T cells in the thymus.

3.3. Increased apoptosis and impaired Akt phosphorylation in dnRac1-Tg mice

The reduced number of DP cells in the thymus of dnRac1-Tg could be a result of increased cell death, therefore we assessed spontaneous and TCR-induced apoptosis of DP cells by Annexin V staining. As shown in Fig. 5A, the proportion of Annexin V positive DP cells was slightly increased in dnRac1-Tg mice, whereas the proportion of apoptotic cells in DN, CD4-SP and CD8-SP cells were not altered. We next investigated the activation of Akt, evaluated by phosphorylation of residue Ser473 in the molecule, because Akt is known to be critical for the survival of DP cells [30–32]. In DP thymocytes, Akt is spontaneously phosphorylated without stimulation [31,33,34] and is further phosphorylated upon TCR-stimulation by anti-CD3 and CD28 antibodies (Fig. 5B). We found that spontaneous phosphorylation of Akt in freshly prepared thymocytes was absent in dnRac1-Tg mice. Furthermore, TCR-stimulation did not induce phosphorylation of Akt phosphorylation in the dnRac1-Tg thymocytes (Fig. 5B). On the other hand, TCR-dependent phosphorylation of Erk was completely normal in dnRac1-Tg thymocytes. From these results, we conclude that Rac GTPases are important for Akt activation with or without TCR stimulation, and thus critical in survival of DP cells, which is consistent with the recent results from a

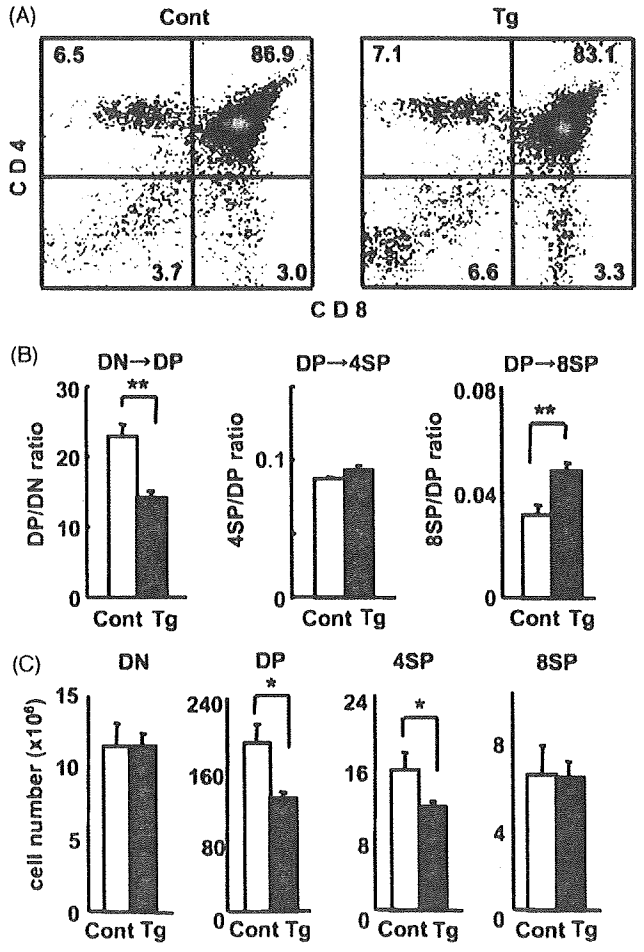

Fig. 2. Development of T cells in the thymus of dnRac1-Tg mice. (A) Thymocytes from 30-day-old dnRac1-tg mice and littermate controls were harvested. Expression of CD4 and CD8 in the thymus was analyzed by flow cytometry. (B) DP/DN, 4SP/DP and 8SP/DP ratios were calculated from analysis of dnRac1-tg mice (Tg) and littermate control mice (Cont). (C) Total cell numbers in DN, DP, CD4-SP and CD8-SP (TCRβhi) populations were calculated. Results are expressed as the mean ± S.E.M. of three independent experiments (Cont, $n = 8$; Tg, $n = 14$).

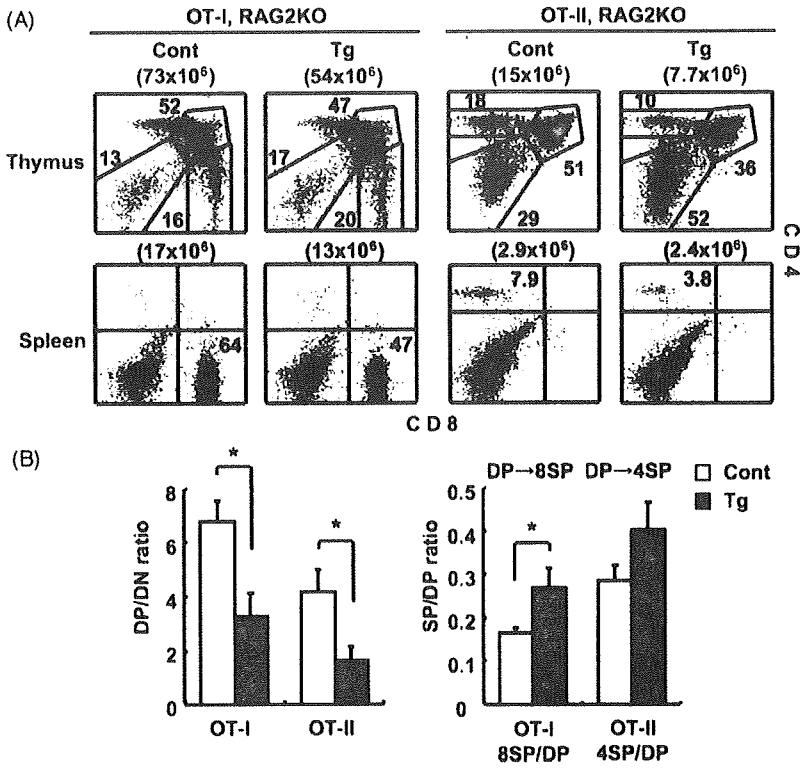

Fig. 3. Thymic selection of dnRac1-Tg expressing class I- and class II-restricted TCR transgenic mice. (A) The expression of CD4 and CD8 in the thymus and spleen of 30-day-old class I- and class II-restricted TCR transgenic, dn-Rac1-Tg mice (Tg) and littermate control mice. (B) DP/DN, 4SP/DN and 8SP/DP ratios of thymocytes were analyzed in class I- and class II-restricted TCR transgenic, dnRac1-tg mice and littermate control mice. The number of mature CD8-SP was calculated from $CD4^-$ $CD8^+$ TCR^{hi} gated cells. Bar graph data are expressed as the mean ± S.E.M. ($n = 3$).

conditional double knockout study of Rac1 and Rac2 in the thymus [22].

3.4. Increased spontaneous apoptosis in peripheral mature T cells

The decrease of mature CD4-SP T cells in periphery was much severer than that in the thymus, and the decrease of CD8-SP T cells was only seen in periphery but not in the thymus. Therefore, reduced numbers of peripheral T cells cannot be explained simply by the impaired survival of DP thymocytes in the thymus. We thus investigated the function of Rac GTPases in peripheral T cells. We first analyzed spontaneous apoptosis of splenic CD4-SP and CD8-SP T cells by the staining of Annexin V. As shown in Fig. 6A, the proportion of Annexin V positive cells of freshly isolated splenic CD4-SP and CD8-SP T cells in dnRac1-Tg mice was significantly increased compared to littermate control mice. At the same time, T cells with lower CD5 expression were significantly increased in dnRac1-Tg splenocytes (Fig. 6B). Since expression of CD5 on T cell is known to correlate well with the strength of TCR signal received [35], this result may indicate that mature T cells in dnRac1-Tg mice received a weaker TCR signal in vivo.

We next investigated Akt activation in splenic CD4-SP T cells. Spontaneous phosphorylation of Akt in splenic CD4-SP T cells without stimulation was reduced in dnRac1-Tg mice (Fig. 6C). Moreover, stimulation dependent phosphorylation of Akt was not detectable in dnRac1-Tg splenic CD4-SP T cells (Fig. 6C). As was seen in DP cells, TCR-induced phosphorylation of ERK was not altered in dnRac1-Tg CD4-SP T cells. These results suggest that Rac GTPases regulate tonic Akt phosphorylation in vivo, and are thus critical for survival of peripheral mature T cells.

3.5. Rac GTPases are required for homeostatic proliferation of mature CD4 T cells, but not for TCR-induced proliferation

We next investigated the effect of Rac GTPases on proliferation of mature T cells. Splenic CD4-SP T cells proliferate when stimulated with plate bound anti-CD3 antibody or a combination of anti-CD3 and anti-CD28 antibodies in vitro. As shown in Fig. 7A and B, TCR-induced proliferation after 3 days was nearly identical in both cell division evaluated by CFSE intensities and MTT assay. On the contrary, when CD4-SP T cells from dnRac1-Tg mice were transferred into lymphopenic $RAG2^{-/-}$ mice, homeostatic proliferation of mature CD4-SP T cells was significantly impaired compared to littermate controls (Fig. 7C). Because IL-7 is known to be critical in homeostatic proliferation under lymphopenic conditions, we next examined the IL-7-dependent survival of dnRac1-Tg T cells. Isolated splenic CD4-SP and CD8-SP T cells were cultured in vitro with or without IL-7 for 7 days and live cells were counted. Survival of both CD4-SP and CD8-SP T cells from dnRac1-Tg in vitro was not altered compared to control littermate (Fig. 7D). Addition of IL-7 in culture media rescued spontaneous cell death in vitro to some extent, however, the IL-7-dependent protective effect was THE same in dnRac1-Tg T cells. Therefore, we concluded that Rac GTPases are not involved in the IL-7 dependent survival of mature T cells. Collectively, these results suggest that Rac GTPases are important for survival and homeostasis of peripheral mature T cells.

4. Discussion

In the present study, we showed impaired generation of DP cells in the thymus and decreased number of peripheral T cells in dnRac1-Tg mice. The role of Rac GTPases in T cell development and activation has not been well characterized. Results from constitu-

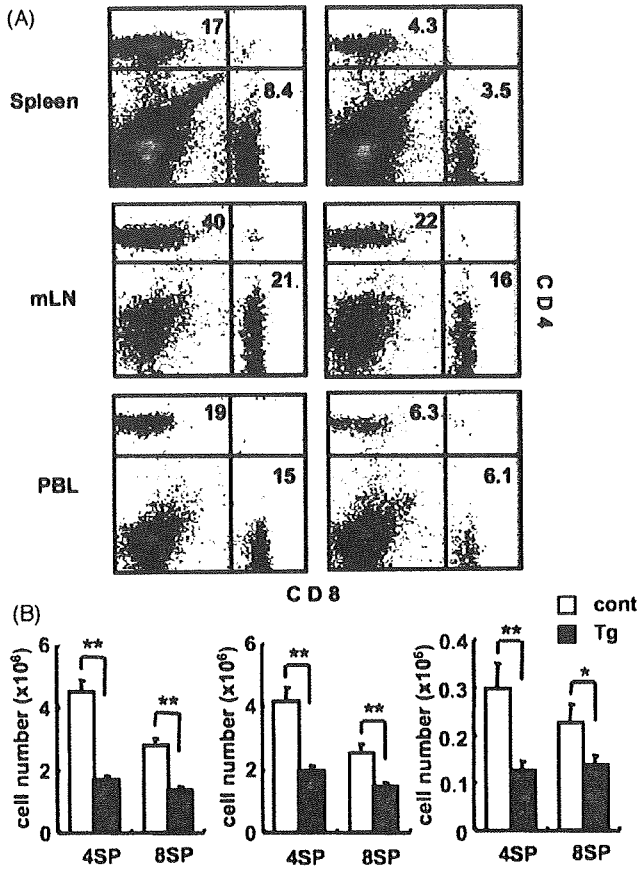

Fig. 4. Number of peripheral T cells is decreased in dnRac1-Tg mice. (A) T cells from spleen, mesenteric lymph node (mLN) and peripheral blood leukocytes (PBL) from 30-day-old dnRac1-Tg mice and littermate control mice were stained with anti-CD4 and anti-CD8 antibodies, and analyzed by flow cytometry. (B) Total cell numbers of CD4-SP and CD8-SP T cells from spleen, mLN and PBL were calculated on the basis of the percentages obtained by flow cytometry. FACS data represent one of four similar experiments for each experimental group. Bar graph of cell numbers are expressed as the mean ± S.E.M. of three independent experiments (Cont, $n = 17$; Tg, $n = 19$). $^{*}p < 0.05$; $^{**}p < 0.01$.

tively active Rac1 transgenic mice showing augmented TCR signal transduction [21], indicated that Rac1 is positively involved in TCR-dependent signal transduction in T cells. Moreover, a study using a DP cell line suggested that positive selection of CD4-SP required Rac1 [26]. From these previous results, we expected that defective Rac GTPases in the thymus would cause inhibition of positive selection.

However, surprisingly, positive selection in the thymus was not impaired in the dnRac1-Tg mice in vivo. Although total numbers of CD4-SP cells generated in the thymus were reduced in dnRac1-Tg mice, the CD4-SP to DP ratio was not altered, suggesting that positive selection of CD4-SP was not affected (Fig. 2). This was also confirmed when we specifically looked at the developmental fate of a class II specific TCR by analyzing the thymi of OT-II TCR Tg-dnRac1-Tg in RAG2$^{-/-}$ mice (Fig. 3). We even observed a slight increase of positive selection in CD8-SP, because the ratio of CD8-SP to DP was increased (Fig. 2). Again, this was also the case for the class I MHC specific OT-I TCR-Tg in RAG$^{-/-}$, dnRac1-Tg mice (Fig. 3). Therefore, reduction of the number of CD4-SP cells in the thymus was due to the reduction of DP cells, but was not due to impaired positive selection in the Tg mice. The reason why positive selection of CD8-SP is increased by inhibition of Rac GTPase activity should be revealed in future study.

Because of limitations in a dominant negative strategy, these phenotypes could be attributed to the insufficient inhibition of Rac GTPase activity (Fig. 1C), or to the unexpected effects by the inhibition of upstream guanine nucleotide exchange factors of Rac1. However, these results are consistent with those in Lck-Cre, Rac1$^{loxp/loxp}$; Rac2$^{-/-}$ mice, which were published recently [22]. Although deletion of either Rac1 alone [22] or Rac2 alone [17] did not affect T cell development, simultaneous deletion of Rac1 and Rac2 in the T cell lineage showed impaired T cell development. In lck-Cre Rac1/Rac2 double knockout (DKO) mice, numbers of total thymocytes were reduced to half, and numbers of CD4-SP cells but not of CD8-SP cells was reduced in the thymus. It was shown that positive selection of CD4-SP was not affected whereas positive selection of CD8-SP was increased. In the periphery of DKO mice, numbers of both CD4-SP and CD8-SP T cells were reduced. These phenotypes are almost identical to the one we saw in our dnRac1-Tg mice. Although we found very weak expression of Rac3 mRNA (Fig. 1A), Rac3 protein was unable to be detected by Western blotting (data not shown), therefore Rac1 and Rac2 are the major Rac GTPases in the thymus, and involvement of Rac3 would be negligible, if it ever exists. This is also consistent with the results that Rac1/Rac2 DKO mice showed similar phenotype to our dnRac1-Tg mice. Very recently, another group reported CD2-Cre driven Rac1/Rac2 DKO mice [23], whose

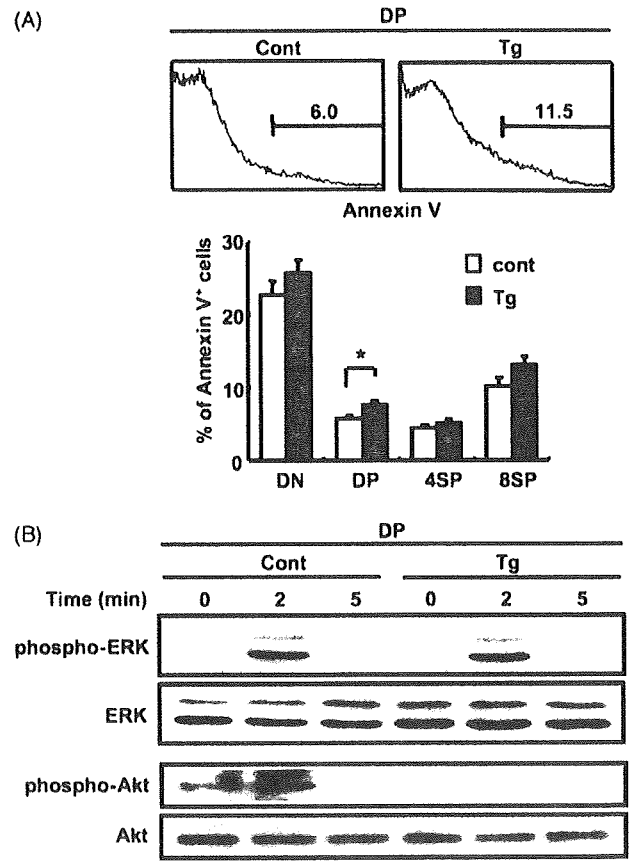

Fig. 5. Increased apoptosis and impaired Akt phosphorylation upon TCR stimulation in dnRac1-Tg DP thymocytes. Thymocytes from 30-day-old dnRac1-Tg mice (Tg) and littermate control mice (Cont) were stained with anti-CD4, anti-CD8 antibodies and Annexin V, and analyzed by flow cytometry. A, FACS data of Annexin V staining represent one of four similar experiments for each experimental group and bar graphs of Annexin V-positive cells were expressed as the mean ± S.E.M. of four independent experiments (Cont, $n = 12$; Tg, $n = 14$). $^{*}p < 0.05$; $^{**}p < 0.01$. (B) Thymocytes isolated from dnRac1-Tg mice were stimulated by anti-CD3 and anti-CD28 antibodies for the indicated periods. Cell lysates were analyzed by Western blotting with antiphospho-ERK, anti-ERK, antiphospho-Akt (Ser473) and anti-Akt antibodies.

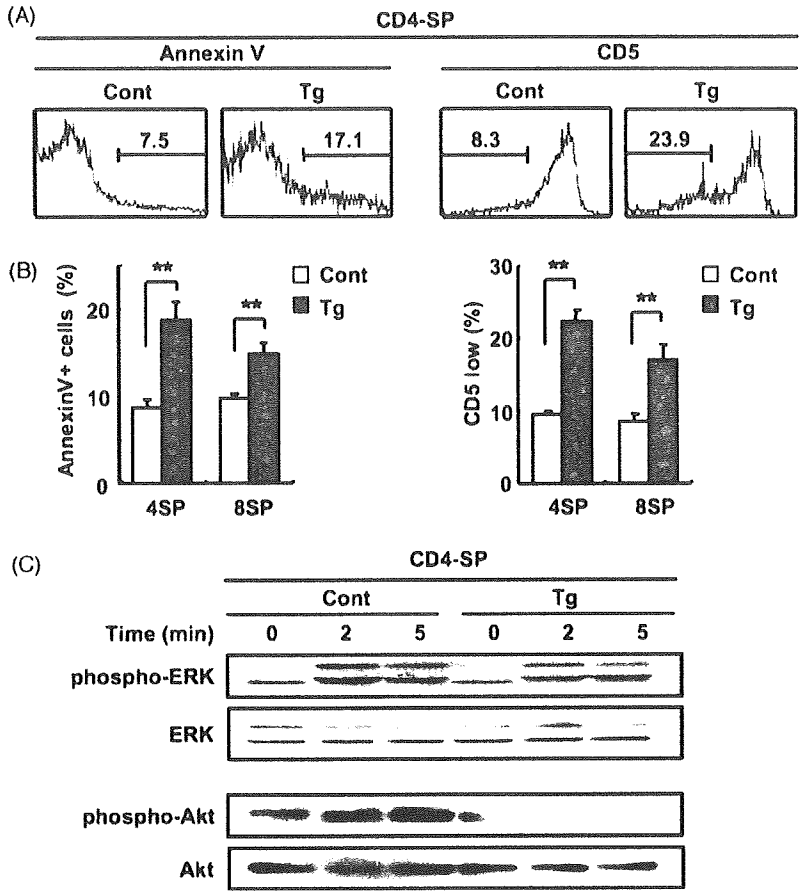

Fig. 6. Increased apoptosis and decreased Akt phosphorylation in dnRac1-Tg splenic T cells. T cells from spleen of 30-day-old dnRac1-Tg mice and nontransgenic littermate controls were stained with anti-CD4, anti-CD8 antibodies and Annexin V or anti-CD5 antibody, and analyzed by flow cytometry. (A) FACS data of Annexin V and anti-CD5 staining represent one of four similar experiments for each experimental group. (B) Bar graphs of indicating the percentage of Annexin V positive cells are expressed as the mean ± S.E.M. of four independent experiments (Cont, $n = 12$; Tg, $n = 14$). (C) Splenic CD4-SP T cells isolated from dnRac1-Tg mice (Tg) and littermate control mice (Cont) were stimulated with anti-CD3 and anti-CD28 antibodies for the indicated periods, and analyzed by Western blotting with antiphospho-ERK, anti-ERK, antiphospho-Akt (Ser473) and anti-Akt antibodies. $^{*}p < 0.05$; $^{**}p < 0.01$.

defect in T cell development was severer and earlier than the one in lck-Cre DKO. Our results is more similar to the phenotype in lck-Cre DKO than the one in CD2 Cre DKO.

We showed impaired spontaneous phosphorylation of Akt in dnRac1-Tg DP cells, and also defective Akt phosphorylation upon TCR stimulation (Fig. 5B). Akt signaling contributes to the differentiation process by promoting the survival of DP T cells [30,31]. This defective Akt activation is consistent with the results from the DKO mice for Rac1 and 2 [22]. These results suggest that the reduced numbers of DP cells seen in dnRac1-Tg mice could be at least partly because of increased cell death caused by impaired activation of Akt. We observed decreased numbers of mature CD4-SP and CD8-SP T cells in the periphery of dnRac1-Tg mice. The number of CD8-SP cells in the thymus was not reduced, and reduction of CD4-SP cells in the thymus was much slighter than that in the periphery, therefore, reduction of both CD4-SP and CD8-SP T cells in the periphery cannot simply be explained by developmental defects in the thymus. We observed increased apoptosis both in CD4-SP and CD8-SP T cells in periphery (Fig. 6A). We also noticed T cells with low CD5 expression were significantly increased in spleens of dnRac1-Tg mice (Fig. 6B), indicating that T cells from these mice received a weaker TCR signal in vivo. Furthermore, we showed that spontaneous activation as well as TCR-induced activation of Akt was severely decreased in dnRac1-Tg peripheral T cells.

Akt is a major downstream target of phosphatidylinositol (PI) 3-kinase signaling which is activated by various stimuli including TCR ligation [36–41]. Akt is activated by TCR stimulation and protects against cell death and regulate cell cycle progression in mature T cells [42]. Therefore, we think a major reason for the severe reduction of peripheral mature T cells in dnRac1-Tg is increased apoptosis caused by impaired Akt activation.

Proliferation and growth of dnRac1-Tg splenic CD4-SP T cells induced by anti-TCR antibody was not reduced in vitro, suggesting that TCR-dependent signal transduction is not seriously affected (Fig. 7A and B). Accordingly, TCR-dependent ERK activation was normal in dnRac1-Tg T cells (Fig. 6C). However, crosslinking of TCR by plate-bound antibody in vitro delivers artificially strong signals, so it may not represent the strength of signaling in vivo. Rac GTPases could be important in weak TCR signaling in vivo. We showed homeostatic proliferation by transferring dnRac1-Tg CD4-SP T cells into lymphopenic $RAG^{-/-}$ mice was significantly reduced compared to control mice. IL-7 and self-MHC molecules on antigen-presenting cells (APCs) play an essential role in the homeostatic expansion of peripheral naive T cells [43–47]. We showed that IL-7-dependent survival of mature T cells in vitro was not altered, suggesting that Rac GTPases are not involved in IL-7-dependent survival signal. Since Rac-dependent chemokine-promoted migration in vivo was shown to be important in homeostatic T cell survival and growth

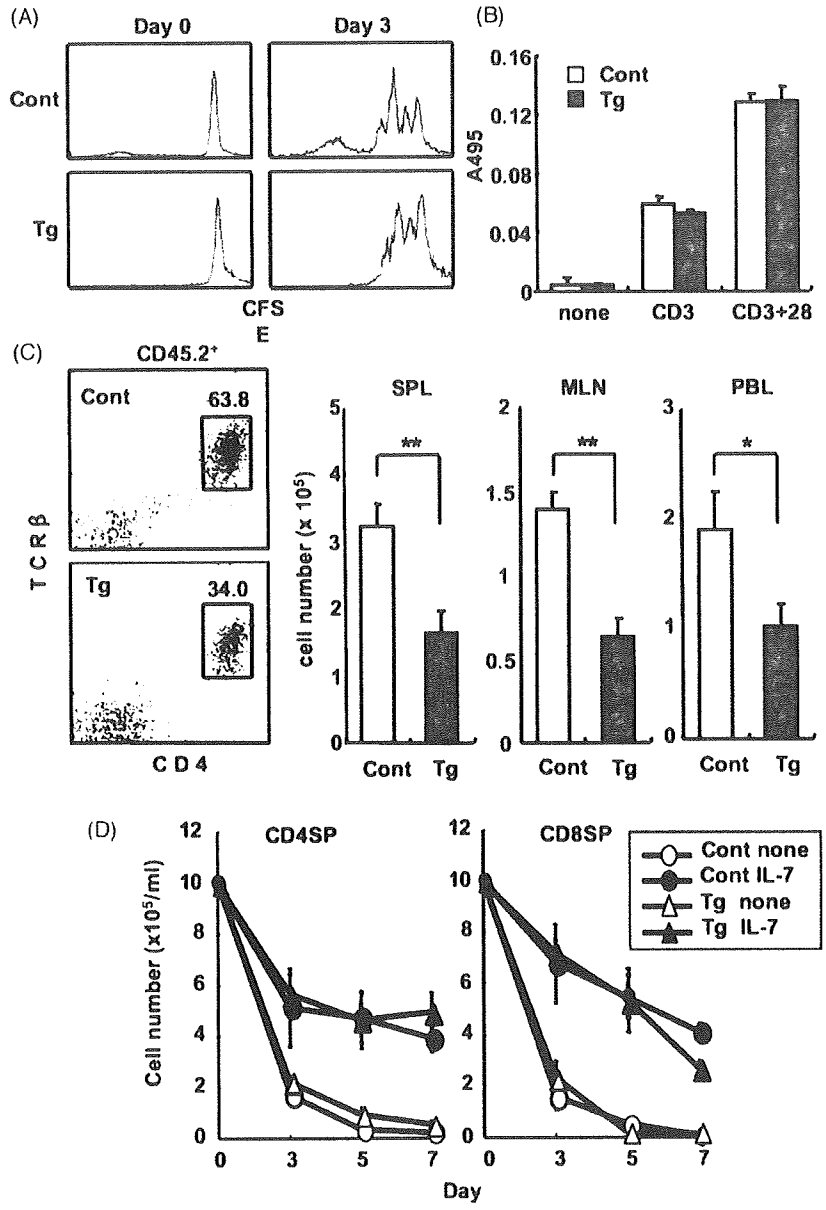

Fig. 7. Proliferation and survival of mature T cells in dnRac1-Tg mice. Splenic CD4-SP T cells were isolated from dnRac1-Tg mice (Tg) and littermate control mice (Cont). (A) CFSE-labeled CD4-SP T cells were stimulated with plate-bound anti-CD3 Ab, and cultured for 3 days. After incubation, cells were analyzed by flow cytometry. (B) After 3 days culture with stimulation, growth of CD4-SP T cells was evaluated by MTT method. (C) CD45.2+CD4-SP T cells from dnRac1-Tg mice and littermate control mice were transferred into CD45.1+RAG2$^{-/-}$ mice. After 40 days, CD45.2+ CD4-SP T cells in spleen, mLN and PBL were analyzed. FACS data represent one of two similar experiments for each group in the spleen. Bar graphs of the number of CD45.2+ CD4-SP cells were calculated on the basis of the percentages obtained by flow cytometry, and results are expressed as the mean ± S.E.M. of two independent experiments ($n = 10$). *$p < 0.05$; **$p < 0.01$. (D) Splenic CD4-SP and CD8-SP T cells were sorted and cultured with or without 1 ng/ml recombinant IL-7 up to 7 days in vitro. Live cells were counted after the indicated period.

[48], it is possible that migration defect would account for impaired T cell survival in vivo.

Collectively, Rac GTPases are important in survival of DP cells and also survival of mature T cells possibly by an Akt-dependent manner. Further analysis of the precise function of Rac in signal transduction of T cells will reveal the significance of Rac GTPases in T cell survival and development.

Acknowledgements

The authors thank Drs. A. Yuo, D. Chida, T. Dohi for technical instructions.

References

[1] Bustelo XR, Sauzeau V, Berenjeno IM. GTP-binding proteins of the Rho/Rac family: regulation, effectors and functions in vivo. Bioessays 2007;29:356–70.
[2] Cantrell DA. GTPases and T cell activation. Immunol Rev 2003;192:122–30.
[3] Scheele JS, Marks RE, Boss GR. Signaling by small GTPases in the immune system. Immunol Rev 2007;218:92–101.
[4] Van Aelst L, D'Souza-Schorey C. Rho GTPases and signaling networks. Genes Dev 1997;11:2295–322.
[5] Gu Y, Filippi MD, Cancelas JA, Siefring JE, Williams EP, Jasti AC, et al. Hematopoietic cell regulation by Rac1 and Rac2 guanosine triphosphatases. Science 2003;302:445–9.
[6] Brenner B, Koppenhoefer U, Weinstock C, Linderkamp O, Lang F, Gulbins E. Fas- or ceramide-induced apoptosis is mediated by a Rac1-regulated activation of Jun N-terminal kinase/p38 kinases and GADD153. J Biol Chem 1997;272:22173–81.

[7] Hall A. Rho GTPases and the actin cytoskeleton. Science 1998;279:509–14.
[8] Arrieumerlou C, Randriamampita C, Bismuth G, Trautmann A. Rac is involved in early TCR signaling. J Immunol 2000;165:3182–9.
[9] Kim C, Dinauer MC. Rac2 is an essential regulator of neutrophil nicotinamide adenine dinucleotide phosphate oxidase activation in response to specific signaling pathways. J Immunol 2001;166:1223–32.
[10] Gomez JC, Soltys J, Okano K, Dinauer MC, Doerschuk CM. The role of Rac2 in regulating neutrophil production in the bone marrow and circulating neutrophil counts. Am J Pathol 2008;173:507–17.
[11] Arana E, Vehlow A, Harwood NE, Vigorito E, Henderson R, Turner M, et al. Activation of the small GTPase Rac2 via the B cell receptor regulates B cell adhesion and immunological-synapse formation. Immunity 2008;28:88–99.
[12] Corbetta S, D'Adamo P, Gualdoni S, Braschi C, Berardi N, de Curtis I. Hyperactivity and novelty-induced hyperreactivity in mice lacking Rac3. Behav Brain Res 2008;186:246–55.
[13] Sugihara K, Nakatsuji N, Nakamura K, Nakao K, Hashimoto R, Otani H, et al. Rac1 is required for the formation of three germ layers during gastrulation. Oncogene 1998;17:3427–33.
[14] Cancelas JA, Lee AW, Prabhakar R, Stringer KF, Zheng Y, Williams DA. Rac GTPases differentially integrate signals regulating hematopoietic stem cell localization. Nat Med 2005;11:886–91.
[15] Jansen M, Yang FC, Cancelas JA, Bailey JR, Williams DA. Rac2-deficient hematopoietic stem cells show defective interaction with the hematopoietic microenvironment and long-term engraftment failure. Stem Cells 2005;23:335–46.
[16] Walmsley MJ, Ooi SK, Reynolds LF, Smith SH, Ruf S, Mathiot A, et al. Critical roles for Rac1 and Rac2 GTPases in B cell development and signaling. Science 2003;302:459–62.
[17] Li B, Yu H, Zheng W, Voll R, Na S, Roberts AW, et al. Role of the guanosine triphosphatase Rac2 in T helper 1 cell differentiation. Science 2000;288:2219–22.
[18] Croker BA, Handman E, Hayball JD, Baldwin TM, Voigt V, Cluse LA, et al. Rac2-deficient mice display perturbed T-cell distribution and chemotaxis, but only minor abnormalities in T(H)1 responses. Immunol Cell Biol 2002;80:231–40.
[19] Yu H, Leitenberg D, Li B, Flavell RA. Deficiency of small GTPase Rac2 affects T cell activation. J Exp Med 2001;194:915–26.
[20] Gomez M, Tybulewicz V, Cantrell DA. Control of pre-T cell proliferation and differentiation by the GTPase Rac-1. Nat Immunol 2000;1:348–52.
[21] Gomez M, Kioussis D, Cantrell DA. The GTPase Rac-1 controls cell fate in the thymus by diverting thymocytes from positive to negative selection. Immunity 2001;15:703–13.
[22] Guo F, Cancelas JA, Hildeman D, Williams DA, Zheng Y. Rac GTPase isoforms, Rac1 and Rac2, play a redundant and crucial role in T-cell development. Blood 2008;112:1767–75.
[23] Dumont C, Corsoni-Tadrzak A, Ruf S, de Boer J, Williams A, Turner M, et al. Rac GTPases play critical roles in early T cell development. Blood 2009;113:3990–8.
[24] Hwang SY, Jung JW, Jeong JS, Kim YJ, Oh ES, Kim TH, et al. Dominant-negative Rac increases both inherent and ionizing radiation-induced cell migration in C6 rat glioma cells. Int J Cancer 2006;118:2056–63.
[25] Marinari B, Costanzo A, Viola A, Michel F, Mangino G, Acuto O, et al. Vav cooperates with CD28 to induce NF-kappaB activation via a pathway involving Rac-1 and mitogen-activated kinase kinase 1. Eur J Immunol 2002;32:447–56.
[26] Oda H, Suzuki H, Sakai K, Kitahara S, Patrick MS, Azuma Y, et al. Rac1-mediated Bcl-2 induction is critical in antigen-induced CD4 single-positive differentiation of a CD4+CD8+ immature thymocyte line. J Leukoc Biol 2007;81:500–8.
[27] Zhumabekov T, Corbella P, Tolaini M, Kioussis D. Improved version of a human CD2 minigene based vector for T cell-specific expression in transgenic mice. J Immunol Methods 1995;185:133–40.
[28] Bolis A, Corbetta S, Cioce A, de Curtis I. Differential distribution of Rac1 and Rac3 GTPases in the developing mouse brain: implications for a role of Rac3 in Purkinje cell differentiation. Eur J Neurosci 2003;18:2417–24.
[29] Melton E, Sarner N, Torkar M, van der Merwe PA, Russell JQ, Budd RC, et al. Transgene-encoded human CD2 acts in a dominant negative fashion to modify thymocyte selection signals in mice. Eur J Immunol 1996;26:2952–63.
[30] Mao C, Tili EG, Dose M, Haks MC, Bear SE, Maroulakou I, et al. Unequal contribution of Akt isoforms in the double-negative to double-positive thymocyte transition. J Immunol 2007;178:5443–53.
[31] Juntilla MM, Wofford JA, Birnbaum MJ, Rathmell JC, Koretzky GA. Akt1 and Akt2 are required for alphabeta thymocyte survival and differentiation. Proc Natl Acad Sci USA 2007;104:12105–10.
[32] Juntilla MM, Koretzky GA. Critical roles of the PI3K/Akt signaling pathway in T cell development. Immunol Lett 2008;116:104–10.
[33] Cunningham NR, Artim SC, Fornadel CM, Sellars MC, Edmonson SG, Scott G, et al. Immature CD4+CD8+ thymocytes and mature T cells regulate Nur77 distinctly in response to TCR stimulation. J Immunol 2006;177:6660–6.
[34] Swat W, Montgrain V, Doggett TA, Douangpanya J, Puri K, Vermi W, et al. Essential role of PI3Kdelta and PI3Kgamma in thymocyte survival. Blood 2006;107:2415–22.
[35] Azzam HS, Grinberg A, Lui K, Shen H, Shores EW, Love PE. CD5 expression is developmentally regulated by T cell receptor (TCR) signals and TCR avidity. J Exp Med 1998;188:2301–11.
[36] Alessi DR, Andjelkovic M, Caudwell B, Cron P, Morrice N, Cohen P, et al. Mechanism of activation of protein kinase B by insulin and IGF-1. EMBO J 1996;15:6541–51.
[37] Gold MR, Scheid MP, Santos L, Dang-Lawson M, Roth RA, Matsuuchi L, et al. The B cell antigen receptor activates the Akt (protein kinase B)/glycogen synthase kinase-3 signaling pathway via phosphatidylinositol 3-kinase. J Immunol 1999;163:1894–905.
[38] Franke TF, Yang SI, Chan TO, Datta K, Kazlauskas A, Morrison DK, et al. The protein kinase encoded by the Akt proto-oncogene is a target of the PDGF-activated phosphatidylinositol 3-kinase. Cell 1995;81:727–36.
[39] Burgering BM, Coffer PJ. Protein kinase B (c-Akt) in phosphatidylinositol-3-OH kinase signal transduction. Nature 1995;376:599–602.
[40] del Peso L, Gonzalez-Garcia M, Page C, Herrera R, Nunez G. Interleukin-3-induced phosphorylation of BAD through the protein kinase Akt. Science 1997;278:687–9.
[41] Reif K, Burgering BM, Cantrell DA. Phosphatidylinositol 3-kinase links the interleukin-2 receptor to protein kinase B and p70 S6 kinase. J Biol Chem 1997;272:14426–33.
[42] Genot EM, Arrieumerlou C, Ku G, Burgering BMT, Weiss A, Kramer IM. The T-cell receptor regulates Akt (protein kinase B) via a pathway involving Rac1 and phosphatidylinositide 3-kinase. Mol Cell Biol 2000;20:5469–78.
[43] Jameson SC. Maintaining the norm: T-cell homeostasis. Nat Rev Immunol 2002;2:547–56.
[44] Broers AEC, Posthumus-van Sluijs SJ, Spits H, van der Holt B, Lowenberg B, Braakman E, et al. Interleukin-7 improves T-cell recovery after experimental T-cell-depleted bone marrow transplantation in T-cell-deficient mice by strong expansion of recent thymic emigrants. Blood 2003;102:1534–40.
[45] Tan JT, Dudl E, LeRoy E, Murray R, Sprent J, Weinberg KI, et al. IL-7 is critical for homeostatic proliferation and survival of naive T cells. Proc Natl Acad Sci USA 2001;98:8732–7.
[46] Clarke SR, Rudensky AY. Survival and homeostatic proliferation of naive peripheral CD4+ T cells in the absence of self peptide:MHC complexes. J Immunol 2000;165:2458–64.
[47] Masse GX, Corcuff E, Decaluwe H, Bommhardt U, Lantz O, Buer J, et al. Gamma(c) cytokines provide multiple homeostatic signals to naive CD4(+) T cells. Eur J Immunol 2007;37:2606–16.
[48] Cinalli RM, Herman CE, Lew BO, Wieman HL, Thompson CB, Rathmell JC. T cell homeostasis requires G protein-coupled receptor-mediated access to trophic signals that promote growth and inhibit chemotaxis. Eur J Immunol 2005;35:786–95.

Lnk regulates integrin αIIbβ3 outside-in signaling in mouse platelets, leading to stabilization of thrombus development in vivo

Hitoshi Takizawa,[1] Satoshi Nishimura,[2,3,4] Naoya Takayama,[5] Atsushi Oda,[6] Hidekazu Nishikii,[5] Yohei Morita,[5] Sei Kakinuma,[5] Satoshi Yamazaki,[5] Satoshi Okamura,[5] Noriko Tamura,[7] Shinya Goto,[7] Akira Sawaguchi,[8] Ichiro Manabe,[2,3,4] Kiyoshi Takatsu,[9] Hiromitsu Nakauchi,[5] Satoshi Takaki,[1] and Koji Eto[5]

[1]Research Institute, International Medical Center of Japan, Tokyo, Japan. [2]Department of Cardiovascular Medicine, Graduate School of Medicine and [3]Translational Systems Biology and Medicine Initiative, University of Tokyo, Tokyo, Japan. [4]PREST, Japan Science and Technology Agency, Tokyo, Japan. [5]Center for Stem Cell Biology and Regenerative Medicine, Institute of Medical Science, University of Tokyo, Tokyo, Japan. [6]Department of Environmental Medicine, Graduate School of Medicine, Hokkaido University, Sapporo, Japan. [7]Department of Medicine, Tokai University School of Medicine, Isehara, Japan. [8]Department of Anatomy, Faculty of Medicine, University of Miyazaki, Miyazaki, Japan. [9]Preferectural Institute for Pharmaceutical Research, Toyama, Japan.

The nature of the in vivo cellular events underlying thrombus formation mediated by platelet activation remains unclear because of the absence of a modality for analysis. Lymphocyte adaptor protein (Lnk; also known as Sh2b3) is an adaptor protein that inhibits thrombopoietin-mediated signaling, and as a result, megakaryocyte and platelet counts are elevated in *Lnk*$^{-/-}$ mice. Here we describe an unanticipated role for Lnk in stabilizing thrombus formation and clarify the activities of Lnk in platelets transduced through integrin αIIbβ3–mediated outside-in signaling. We equalized platelet counts in wild-type and *Lnk*$^{-/-}$ mice by using genetic depletion of Lnk and BM transplantation. Using $FeCl_3$- or laser-induced injury and in vivo imaging that enabled observation of single platelet behavior and the multiple steps in thrombus formation, we determined that Lnk is an essential contributor to the stabilization of developing thrombi within vessels. *Lnk*$^{-/-}$ platelets exhibited a reduced ability to fully spread on fibrinogen and mediate clot retraction, reduced tyrosine phosphorylation of the β3 integrin subunit, and reduced binding of Fyn to integrin αIIbβ3. These results provide new insight into the mechanism of αIIbβ3-based outside-in signaling, which appears to be coordinated in platelets by Lnk, Fyn, and integrins. Outside-in signaling modulators could represent new therapeutic targets for the prevention of cardiovascular events.

Introduction

Platelet activation is controlled through a series of highly regulated processes and is critical for maintaining normal homeostasis (1). The nature of hemostasis and thrombosis mediated in vivo by activated platelets and its contribution to cardiovascular events remains unclear, however. Particularly challenging has been the characterization of the multicellular network of interactions among platelets, endothelial cells, leukocytes, and erythrocytes that occur during thrombus formation in pathological settings and analysis of the kinetics of platelet activity. Injury to vascular endothelial cells exposes matrix proteins, which induce platelets to adhere to the vessel wall, where they subsequently spread and become activated. At the high shear rates found within the circulation, vWF immobilized on the vessel wall binds to the platelet receptor glycoprotein Ib-V-IX complex (GPIb-V-IX), facilitating platelet adhesion to injured sites, where collagen and/or laminin are exposed (2, 3). Once activated, the adhering platelets secrete soluble mediators to recruit additional circulating platelets, and, through their aggregation, bleeding is stopped. Platelet activation is mediated via several signaling pathways, including the integrin αIIbβ3 pathway (1). Other receptor-ligand interactions, including the binding of GPVI-collagen, $P2Y_1$/$P2Y_{12}$-ADP, and protease-activated G protein–coupled receptor–thrombin (PAR-thrombin), synergistically promote integrin αIIbβ3 activation (inside-out signaling) and the subsequent binding of fibrinogen or vWF to integrin αIIbβ3. This binding triggers signaling that promotes cytoskeletal changes that lead to the spread and stabilization of platelet thrombi through a process termed outside-in signaling (1, 2).

It is also known that αIIbβ3 physically interacts with non-receptor tyrosine kinases such as Src and Syk (4, 5) and that activation of these kinases upon engagement of integrin with fibrinogen contributes to the stability of thrombi in vivo (6). The kinases and adaptors involved in the assembly of the αIIbβ3-based signaling complex are believed to include Syk, lymphocyte cytosolic protein 2 (Lcp2, also known as SH2 domain–containing leukocyte protein of 76 kDa [SLP-76]), Vav, and Fyn-binding protein (Fyb, also known as adhesion and degranulation promoting adaptor protein [ADAP]) (4, 5). Tyrosine phosphorylation of the cytoplasmic domain of the integrin β3 subunit, at least on Tyr747, is required for stable platelet aggregation and the interaction of myosin with the β3 subunit in platelets (7), which is believed to be necessary for full clot retraction (8–10).

Lnk (SH2B adaptor protein 3 [Sh2b3]) belongs to the Src-homology 2 (SH2) adaptor family, which also includes SH2-B (Sh2b1) and adaptor protein with PH and SH2 domains (APS; Sh2b2) (11).

Authorship note: Hitoshi Takizawa and Satoshi Nishimura contributed equally to this work.

Conflict of interest: The authors have declared that no conflict of interest exists.

Citation for this article: *J. Clin. Invest.* doi:10.1172/JCI39503.

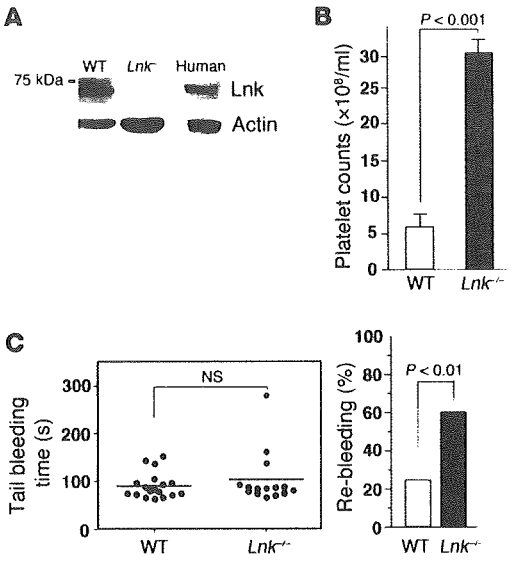

Figure 1
Increased numbers of platelets circulate in *Lnk*$^{-/-}$ mice, but re-bleeding events are increased, while bleeding times are comparable. (**A**) Lnk levels in platelets. Washed platelets from WT and *Lnk*$^{-/-}$ mice or human platelets were lysed and were subjected to immunoblotting with anti-Lnk and anti-actin Abs. (**B**) Platelet counts in EDTA-treated peripheral blood (mean ± SD, n = 15 each). (**C**) Tails of WT (n = 18) and *Lnk*$^{-/-}$ mice (n = 15) were warmed and then transected, immersed in PBS at 37°C, and then monitored for 60 seconds so that any re-bleeding would be detected (detection was positive or negative). Horizontal bars in the left panel show mean in each group.

Lnk-deficient (*Lnk*$^{-/-}$) mouse strains exhibit excessive accumulation of c-Kit$^+$Sca-1$^+$lineage$^-$ (KSL) CD34^{low} HSCs, B cell precursors, erythroblasts, megakaryocytes, and platelets but do not exhibit thrombogenesis and have normal longevity (11–14). The observed phenotypes of *Lnk*$^{-/-}$ mice are caused by a loss of negative regulation by Lnk signaling transduced through several growth factor and cytokine receptors, including the stem cell factor receptor c-Kit, the erythropoietin receptor, and the thrombopoietin receptor c-Mpl (11, 12, 14–17). In the present study, we used an $FeCl_3$-induced injury model and our high-resolution imaging system, which enables observation of single platelet behavior in vivo (18), to examine the function of Lnk in platelets with the aim of clarifying its role in thrombosis. Our results suggest that Lnk promotes stabilization of the developed thrombus, mainly through integrin αIIbβ3-mediated actin cytoskeletal reorganization, and suggest this molecule may represent a new therapeutic target for the treatment and/or prevention of cardiovascular disease.

Results

Thrombus stability is impaired in Lnk$^{-/-}$ *mice in different mouse models of thrombosis.* Lnk is expressed by megakaryocytes, where it acts through integrin signaling to regulate their growth and maturation (14, 19). To determine whether platelets retain Lnk after their release from megakaryocytes and, if so, what its function is, we first used immunoblotting to assess Lnk levels in platelets obtained from WT C57BL/6 mice. This analysis confirmed that substantial amounts of Lnk are retained by WT platelets, and similar results were obtained in humans (Figure 1A). Accordingly, we next investigated the function of Lnk in platelets by examining the effect of Lnk deficiency. As reported previously (14, 19), *Lnk*$^{-/-}$ mice showed a 5-fold increase in platelet number (Figure 1B), though flow cytometry revealed platelet size to be unaffected by the absence of Lnk (data not shown). Moreover, transmission electron microscopic examination revealed that the intracellular structures of resting WT and *Lnk*$^{-/-}$ platelets, including the α- and dense granules, were indistinguishable (Supplemental Figure 1A; supplemental material available online with this article: doi:10.1172/JCI39503DS1). Likewise, the expression levels of the major integrin subunits, αIIb, α2, β3, and β1, as well as GPIbα (the vWF receptor) and GPVI (the collagen receptor), were also similar in WT and *Lnk*$^{-/-}$ platelets (Supplemental Figure 1B).

To examine the functional consequences of Lnk deficiency in mice, we inflicted tail wounds on the mice, after which *Lnk*$^{-/-}$ mice exhibited bleeding times that were comparable to those in WT mice. But whereas 23% of WT mice showed re-bleeding, 60% of *Lnk*$^{-/-}$ mice re-bled ($P < 0.01$ in a χ^2 test, Figure 1C; re-bleeding times did not differ significantly: WT, 58 ± 8 seconds vs. *Lnk*$^{-/-}$, 62 ± 6 seconds), suggesting that thrombi formed in *Lnk*$^{-/-}$ mice are more fragile than those formed in WT mice (1, 8, 20).

To accurately interpret the results summarized above, 2 characteristics of the system had to be taken into account: (a) the numbers of circulating platelets in *Lnk*$^{-/-}$ mice were 5-fold higher than in WT mice (Figure 1B); and (b) Lnk is expressed in endothelial cells as well as platelets (21). In order to exclude the influence of endothelial cells and platelet number, we performed BM transplantation using WT or *Lnk*$^{-/-}$ BM cells. Because it is well established that Lnk deficiency increases stem cell number and enhances the engraftment efficiency upon transplantation (22), we transplanted 1×10^7 BM cells from Ly5.1 WT mice or 2×10^5 or 5×10^5 BM cells from Ly5.1 *Lnk*$^{-/-}$ mice into irradiated 8-week-old Ly5.2 recipient mice, which are hereafter referred to as WT-chimeras and Lnk-chimeras, respectively (Figure 2A). We confirmed that with successful BM replacement (all mice used showed greater than 98% chimerism at Ly5.1/Ly5.2 on myeloid-lineage cells) and with platelets lacking Lnk expression from Lnk-chimeras, the platelet counts in 16-week-old WT-chimeras (8 weeks after transplantation) were comparable to those in 12-week-old Lnk-chimeras (4 weeks after transplantation). By 8 weeks after transplantation, the Lnk-chimeras showed higher platelet counts (Figure 2B). Correspondingly, when compared with WT-chimeras at 8 weeks after transplantation, bleeding times were significantly prolonged in Lnk-chimeras at 4 weeks but not at 8 weeks ($P < 0.01$, Figure 2B). WT-chimeras at 8 weeks, Lnk-chimeras at 4 weeks, and Lnk-chimeras at 8 weeks showed re-bleeding times of 59 seconds (3 of 14 mice), 246 seconds (7 of 14 mice), and 57 seconds (5 of 11 mice), respectively. This suggests that the Lnk deficiency itself contributes to the increased tail bleeding and re-bleeding times. Although there was a high inverse correlation between bleeding times and platelet counts in both

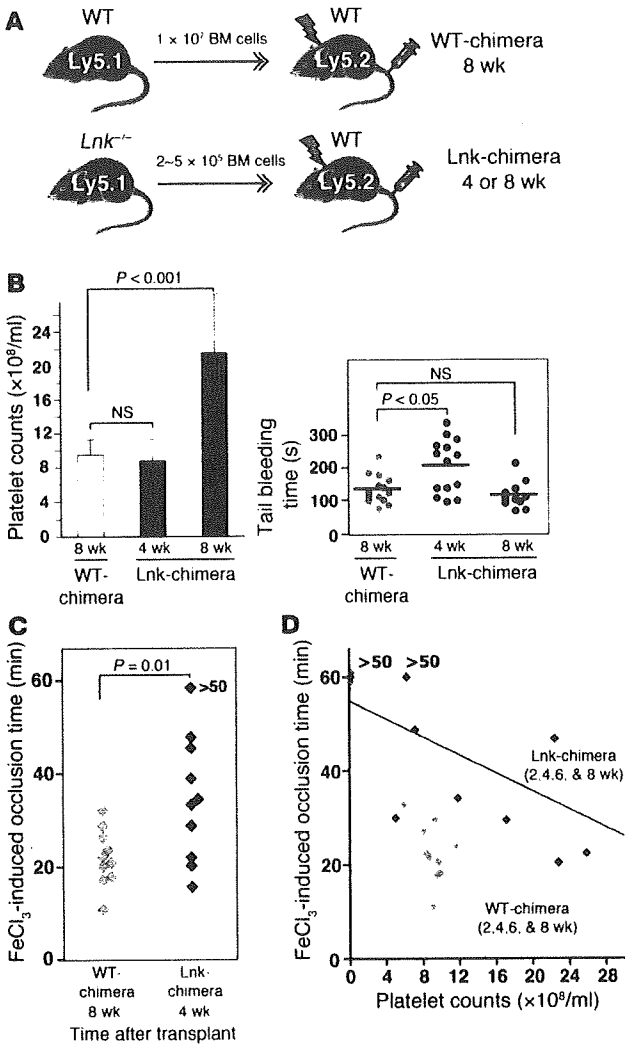

Figure 2
Adjustment of platelet counts through BM transplantation showed prolonged bleeding and occlusion times in a $FeCl_3$-induced thrombosis model. (**A**) The protocol for BM transplantation. (**B**) The left panel shows the platelet counts after transplantation (n = 11–14); data represent mean ± SD. The right panel shows the duration of tail bleeding at the indicated time points; horizontal bars show mean in each group. (**C**) Platelet counts in BM-transplanted mice. WT-chimeras at 8 weeks and Lnk-chimeras at 4 weeks after transplantation were utilized to measure occlusion times during $FeCl_3$-induced thrombosis in carotid arteries (WT-chimera, n = 10; Lnk-chimera, n = 10; P = 0.01). (**D**) Relationship between occlusion times with $FeCl_3$-induced thrombosis and platelet counts in WT- and Lnk-chimeras measured 2, 4, 6, and 8 weeks after transplantation (n = 12 animals in each group). Black symbols denote Lnk-chimeras, while gray ones denote WT-chimeras; the black ($y = -0.96x + 55.0$) and gray lines ($y = -3.94x + 58.6$) are fitted to the data from the Lnk- and WT-chimeras, respectively.

WT- and Lnk-chimeras, irrespective of platelet age or circulating platelet counts (Supplemental Figure 2), the results again suggest that the impaired thrombosis reflects the Lnk deficiency.

We then evaluated occlusion times in carotid arteries exposed to $FeCl_3$ (10% solution on the adventitial side) to induce endothelial injury for assessing thrombus formation in vivo (23). We found that in WT- and Lnk-chimeras with comparable platelet counts, occlusion times were significantly longer in the Lnk-chimeras, which is also indicative of a functional defect in *Lnk*$^{-/-}$ platelets (WT-chimera, n = 10; Lnk-chimera, n = 10; P = 0.01, Figure 2C). When we analyzed for the relationship between occlusion times and platelet counts in the chimeras 2, 4, 6, and 8 weeks after transplantation, there was a high inverse correlation between occlusion times and platelet counts. Of note, however, Lnk-chimeras exhibited longer occlusion times than WT-chimeras with similar platelet counts (Figure 2D), further confirming that Lnk deficiency impairs thrombus formation.

To assess the functionality of *Lnk*$^{-/-}$ platelets in more detail, we used a direct visual technique that enabled us to evaluate in vivo thrombus stability with much greater temporal and spatial resolution and to characterize the kinetics of *Lnk*$^{-/-}$ platelet activity involved in thrombus formation. This method is based on confocal laser microscopy and permits high spatiotemporal resolution of individual platelets under flow conditions in mesenteric capillaries and arterioles (24). With this system, laser irradiation produces ROS, which cause injury to the endothelial layer of the vessels (18). Because laser-induced thrombosis reportedly differs from the $FeCl_3$-induced injury model in terms of the mechanism of thrombus formation (25, 26), we again used WT-chimeras 8 weeks after transplantation and Lnk-chimeras 4 weeks after transplantation, as we did in the experiments shown in Figure 2C. We found that WT- and Lnk-chimeras showed similar single platelet kinetics in the absence of injury, including transient interactions with the endothelium (data not shown). After laser-induced injury, however, thrombus formation was severely diminished in the Lnk-chimeras.

After laser-induced injury to mesenteric capillaries, platelets adhered to the vessel walls at similar rates in the WT- and Lnk-chimeras (WT-chimeras, 1.59 ± 0.18 platelets/ms/μm vs. Lnk-chimeras, 1.48 ± 0.19 platelets/ms/μm; n = 30 vessels from 5 animals, P = 0.44). In the WT-chimeras, the adherent platelets caused platelets in the flowing blood to acutely pile up, and the resultant thrombus reduced the vessel lumen diameter and blood flow velocity. Ultimately, the blood vessel was completely occluded by plugged erythrocytes and/or leukocytes. By contrast, in the Lnk-chimeras, platelets adhered to the vessel wall more loosely than in WT-chimeras, so that they were frequently washed away by the blood flow. As a consequence, the number of platelets that piled up and the size of the resultant thrombus were smaller than in WT-chimeras (Figure 3A and Supplemental Videos 1 and 2). More intriguingly, in both Lnk- and WT-chimeras 2, 4, 6, and 8 weeks after transplantation, the number of platelets adhering to the vessel walls during thrombus formation appeared to be well correlated with the circulating platelet count. However, when we compared thrombus formation in Lnk- and WT-chimeras with similar platelet counts, there was a tendency for animals with *Lnk*$^{-/-}$ platelets (Lnk-chimeras) to show impaired thrombus formation, as compared with WT-chimeras. Moreover, the greatly increased platelet numbers in *Lnk*$^{-/-}$ animals did not enhance thrombus formation to levels similar to those seen in WT-chimeras (Figure 3B), which suggests that Lnk deficiency is itself a factor that contributes to the impaired stabilization of developing thrombi in our laser-induced injury model.

We also applied the laser-induced injury model to compare thrombosis in mesenteric capillaries and arterioles of 12-week-old

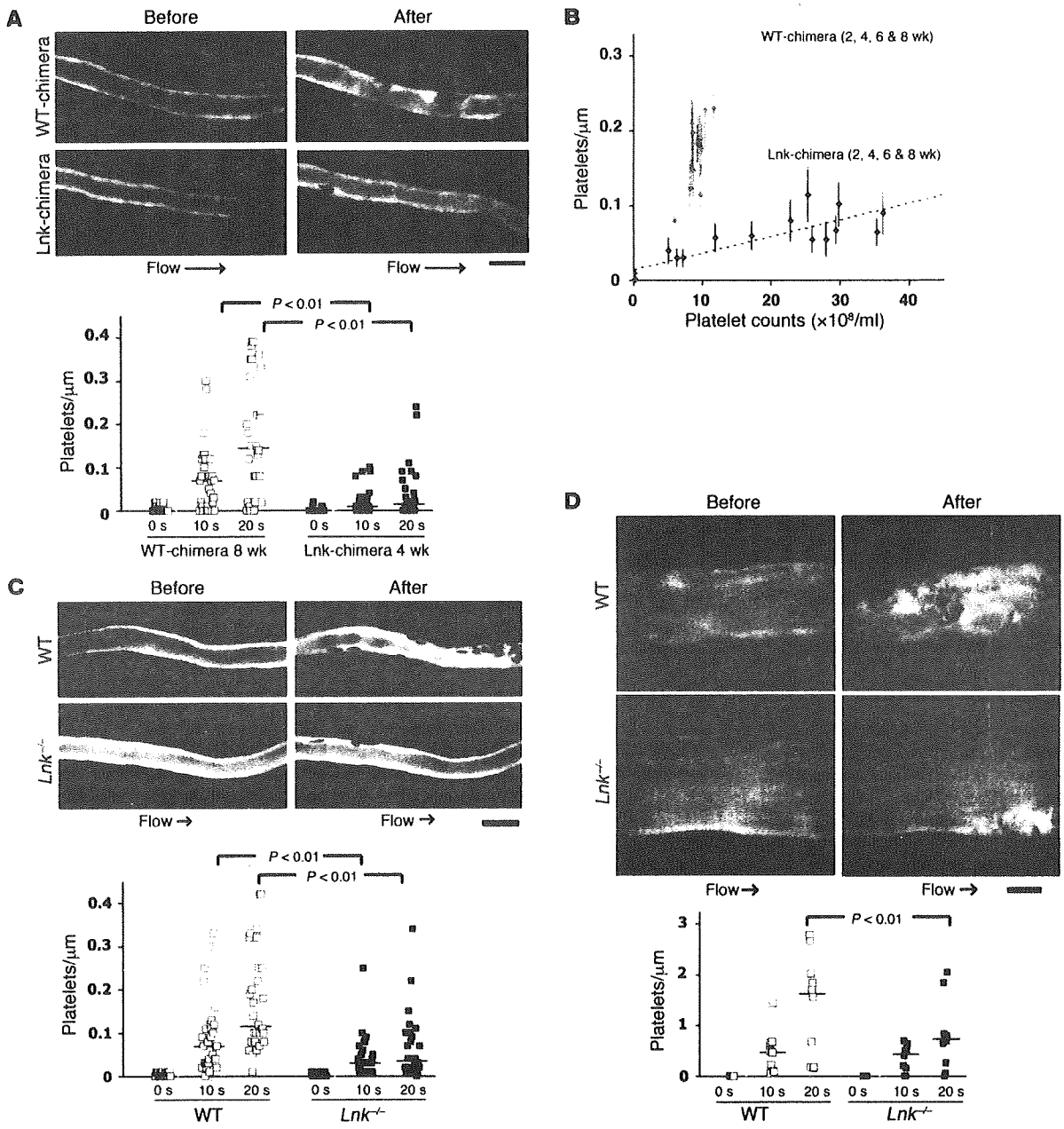

Figure 3

In vivo thrombus formation was impaired in Lnk-chimeras and *Lnk*$^{-/-}$ mice in a laser-induced injury model. (**A**, **C**, and **D**) Video stills of mesenteric capillaries (**A** and **C**) and arterioles (**D**) obtained using intravital fluorescence microscopy before and 20 seconds after laser-induced injury. The numbers of platelets in developing thrombi after laser injury to capillaries (**A** and **C**, lower panel) and arterioles (**D**, lower panel) were calculated. In **A**, **C**, and **D**, *y* axes represent the numbers of platelets per micrometer of observed vessel length. In **A**, results from WT-chimeras 8 weeks after transplantation (16 weeks old) and Lnk-chimeras 4 weeks after transplantation (12 weeks old) are shown ($n = 5$ each). (**B**) Relationship between platelet counts and laser-induced thrombosis. All recipient mice were studied 2, 4, 6, or 8 weeks after transplantation ($n = 17$ animals for each groups). For each mouse, the numbers of platelets per micrometer contributing to thrombi after 20-second injuries to 10 mesenteric capillaries are shown as mean ± SEM along with platelet count. Black and gray dotted lines are fitted to the data from the Lnk- and WT-chimeras, respectively. (**C** and **D**) Results from 12-week-old WT and *Lnk*$^{-/-}$ mice ($n = 5$ each). See Supplemental Videos 1–6 for original movies. Note the impaired thrombus formation in *Lnk*$^{-/-}$ mice in both capillaries and arterioles. Scale bars: 10 μm. Horizontal lines indicate the median values in **A**, **C**, and **D**.

WT and *Lnk*$^{-/-}$ mice (Figure 3, C and D, for capillaries and arterioles, respectively). Upon laser-induced injury, the platelet kinetics in *Lnk*$^{-/-}$ mice were similar to those seen in the Lnk-chimeric mice 4 weeks after transplantation. Initial attachment of the platelets to the vessel wall was observed; however, stable thrombus formation, including the piling up of platelets, was diminished in manner similar to that seen in the Lnk-chimeras. As a result, the numbers of platelets making up the thrombi were significantly reduced in

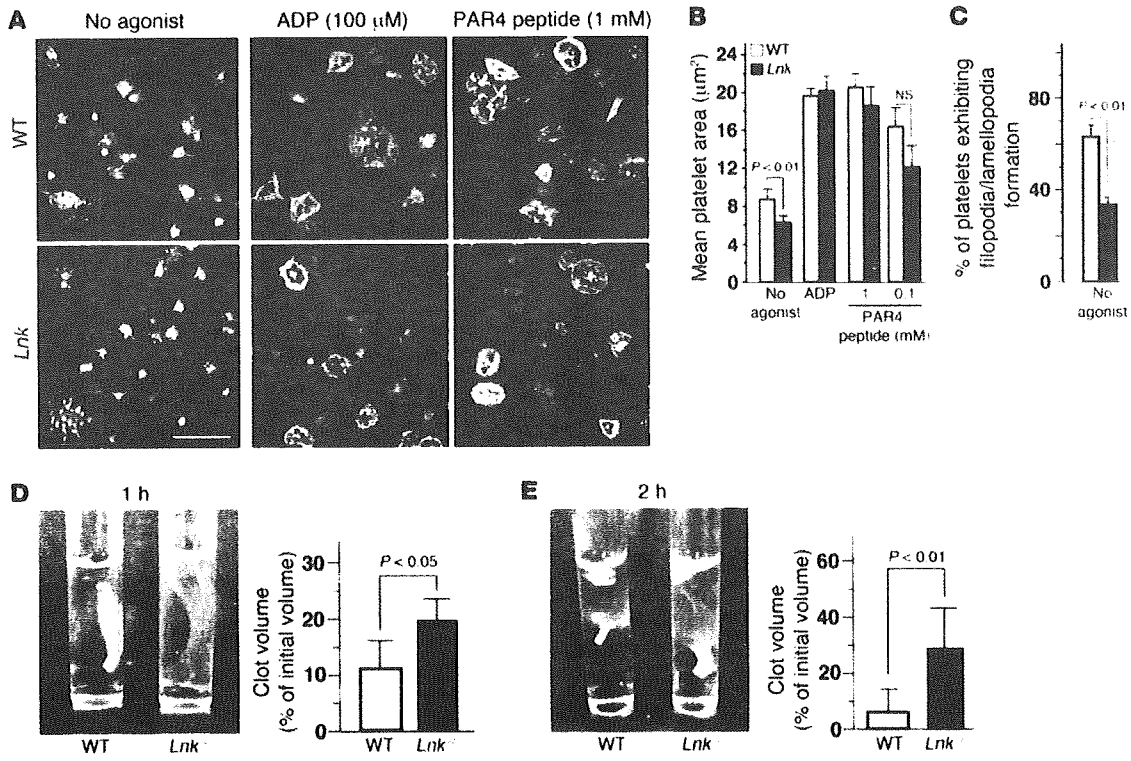

Figure 4

Lnk$^{-/-}$ platelets show defective αIIbβ3-dependent spreading on fibrinogen and fibrin clot retraction. (**A**) Washed platelets from WT and *Lnk*$^{-/-}$ mice were plated on fibrinogen-coated coverslips for 45 minutes. In some preparations, 100 μM ADP or 0.1 or 1 mM PAR4 receptor–activating peptide was present. Cells were fixed, permeabilized, and stained with rhodamine-phalloidin to visualize F-actin (red) and with anti-phosphotyrosine mAb (green). Scale bars: 10 μm (white); 4 μm (insets, orange). (**B**) Platelet spreading was quantified by computer analysis of their surface areas. Each bar in **B** represents the value (mean ± SD) from at least 250 platelets. (**C**) Percentages of platelets exhibiting filopodia or lamellipodia. Twenty sections (20–30 cells/section) were analyzed, and mean ± SD is shown. (**D** and **E**) Fibrin clot retraction was assessed at 1 and 2 hours after addition of thrombin, fibrinogen, and $CaCl_2$ to washed platelets from WT or *Lnk*$^{-/-}$ mice. The images show representative results at 1 (**D**) and 2 hours (**E**). The graphs show the summarized results at 1 (**D**) and 2 hours (**E**) (mean ± SD, n = 10 each).

both mesenteric capillaries (Figure 3C and Supplemental Videos 3 and 4) and arterioles (Figure 3D and Supplemental Videos 5 and 6). Taken together, the results indicate that the observed phenotype for thrombus formation caused by the Lnk deficiency is attributable to platelet function, per se, and does not reflect changes in endothelial cell function. This is noteworthy, as it suggests that there could be less thrombus formation in the Lnk-chimeras than in *Lnk*$^{-/-}$ mice, as the higher platelet counts in the latter might slightly compensate for their diminished functionality (Figure 3, A–C).

Lnk promotes integrin αIIbβ3-mediated actin cytoskeletal reorganization but not agonist-dependent integrin activation. To determine the basis for the instability of thrombi formed by *Lnk*$^{-/-}$ platelets, we examined their ability to adhere to fibrinogen-coated plates and their morphology after spreading, both of which are dependent on outside-in αIIbβ3 signaling (1, 8, 27). The initial adhesion of *Lnk*$^{-/-}$ platelets to fibrinogen-coated plates in the absence of agonistic stimuli appeared normal, as did formation of filopodial projections (data not shown). On the other hand, their subsequent spreading (after 15 minutes) was impaired, and formation of a lamellipodial edge was incomplete (shown at 45 minutes, Figure 4A, "No agonist") (28, 29). The mean area covered by the adhering platelets and the percentage of platelets showing filopodia and/or lamellipodia (percentage of spreading) were both significantly reduced in the absence of Lnk (at 45 minutes, Figure 4, B and C; time-dependent change in mean area without agonist, Supplemental Figure 3A). This suboptimal spreading of *Lnk*$^{-/-}$ platelets was not observed when they were stimulated with a high concentration of a G protein–coupled receptor agonist such as 100 μM ADP or 1 mM PAR4-activating peptide (sequence: AYPGKF) (Figure 4, A and B), although lower concentrations of agonists, such as 0.1 mM PAR4-activating peptide (Figure 4B) or 0.05 U/ml thrombin (Supplemental Figure 3B), did not completely restore the spreading on immobilized fibrinogen impaired by Lnk deficiency, even when the secretion of effectors from platelet granules was blocked (Supplemental Figure 3B). In addition, there was no significant difference in the reduction in the spread areas of platelets from Lnk-chimeras 4 weeks and 8 weeks after transplantation (data not shown), indicating that the impaired spreading caused by Lnk deficiency is independent of platelet age after myelosuppression. Thus, Lnk appears to continuously participate in a subset of αIIbβ3- and actin-dependent morphological responses triggered by platelet adhesion to fibrinogen (1) independently of its negative impact on proliferation in HSCs and megakaryocytes (12, 14, 19).

Another platelet response that is dependent on αIIbβ3 and the actin cytoskeleton is fibrin clot retraction (8, 9, 27), which we examined using equal numbers of *Lnk*$^{-/-}$ and WT washed platelets

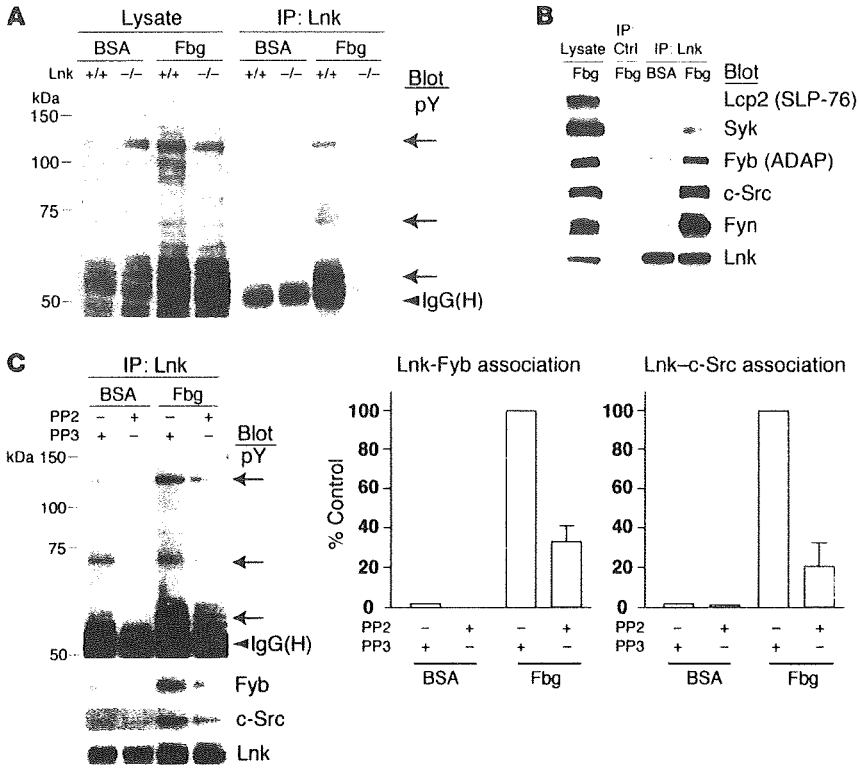

Figure 5

Lnk associates with c-Src, Fyn, and Fyb in a manner dependent on outside-in signaling. (**A**) Washed platelets from WT and *Lnk*$^{-/-}$ mice were plated on fibrinogen (Fbg) for 45 minutes or maintained in suspension in a BSA-coated dish. Platelet lysate (left) or proteins immunoprecipitated using anti-Lnk Abs (right, IP: Lnk) were separated and probed with anti-phosphotyrosine (pY) mAb. (**B**) Lysates from WT platelets prepared as in **A** and immunoprecipitates obtained using irrelevant control rabbit sera (IP: Ctrl) or anti-Lnk (IP: Lnk) were probed by immunoblotting for the indicated proteins. (**C**) WT platelets were incubated with 5 μM PP2 to block Src kinase activity or with PP3, an inactive congener of PP2. PP2 but not PP3 diminished tyrosine phosphorylation of cellular proteins and the association of c-Src and Fyb, with Lnk in platelets adhering to fibrinogen. The observation was confirmed using 20 μM SU6656, an unrelated selective c-Src inhibitor (data not shown). Arrows indicate bands for the expected phosphoproteins corresponding to Fyb, Lnk, and c-Src. Results shown are representative of 3 independent experiments. The 2 panels on the right show the quantification of Western blot bands from 3 experiments (mean ± SD). Maximal band density was defined as 100%.

in the presence of fibrinogen, $CaCl_2$, and thrombin (Figure 4, D and E). Under these conditions, the clot retraction seen with *Lnk*$^{-/-}$ platelets was slower and less effective than that seen with WT platelets, which is consistent with the idea that platelet responses are dependent on αIIbβ3-mediated actin cytoskeletal signaling and that Lnk is involved. To further study the role of αIIbβ3 activation in *Lnk*$^{-/-}$ platelets, we also used flow cytometry to quantify the specific binding of Alexa Fluor 488–conjugated fibrinogen to washed platelets upon stimulation with various concentrations of ADP, epinephrine, PAR4 peptide, phorbol myristate acetate, or convulxin (CVX), which selectively stimulates GPVI (Supplemental Figure 4A). We found that *Lnk*$^{-/-}$ and WT platelets showed similar fibrinogen binding, irrespective of the agonist inducing the inside-out signaling. In addition, levels of P-selectin expression were indistinguishable (Supplemental Figure 4B), suggesting that Lnk is not involved in α-granule secretion.

Lnk recruitment to the αIIbβ3-based signaling complex is dependent on outside-in signaling and c-Src activation. To understand the mechanism by which Lnk regulates outside-in signaling, we sought the molecule(s) that associates with Lnk in platelets. One prominent cellular event required for integrin-dependent responses is tyrosine phosphorylation of several cytosolic proteins (Figure 5A) (1, 4, 27). Incubation of WT platelets on fibrinogen induced tyrosine phosphorylation of cellular proteins with molecular weights of 60, 65–75, 90–110, and 120–130 kDa, but much less post-engagement tyrosine-phosphorylation was seen in *Lnk*$^{-/-}$ platelets. In addition, immunoprecipitation assays revealed that several phosphoproteins associate with Lnk (the 68-kDa protein was likely Lnk itself). A variety of proteins, including Syk, LCP2, and Fyb, are known to be tyrosine phosphorylated in an Src-dependent manner in fibrinogen-adherent platelets (29, 30). In the present study, both c-Src and Fyb co-immunoprecipitated with Lnk from WT platelets adhering to fibrinogen but not from unstimulated ones; Syk was only weakly detectable, and LCP2 was barely so (Figure 5B). It has also been proposed that Fyn, an Src-family protein, may contribute to integrin αIIbβ3 signaling (9, 20), and we found that, like c-Src, Fyn associated with Lnk in stimulated platelets (Figure 5B).

c-Src and Fyn are known to associate with the cytoplasmic tail of the integrin β3 subunit in vitro (20, 31), which suggests that after platelets bind to fibrinogen, Lnk regulates the assembly of an αIIbβ3-based signaling complex (5). We therefore asked whether the observed association of c-Src and/or Fyb with Lnk is dependent on Src kinase activity. When platelets were incubated with 5 μM PP2 (to block Src kinase activity) or PP3 (an inactive congener of PP2), PP2 but not PP3 diminished tyrosine phosphorylation of cellular proteins and the association of c-Src and Fyb with Lnk in platelets adhering to fibrinogen (Figure 5C). To then confirm that the phosphorylation of Lnk and its association with c-Src are dependent on c-Src activation, we used a COS7 cell expression system to evaluate the interaction in more detail (Supplemental Figure 5A). Flag-tagged WT Lnk (WT-Lnk) or a mutant form lacking the C-terminal portion containing Tyr536 (ΔC-Lnk) was expressed in COS7 cells in the presence and absence of a constitutively active form of human c-Src (Y530F, CA-Src). Whereas WT-Lnk became tyrosine phosphorylated when coexpressed with CA-Src, ΔC-Lnk showed little or no phosphorylation, indicating that Tyr536 is a key target site for phosphorylation by c-Src (Supplemental Figure 5A). On the other hand, a constitutively active form of Fyn did not phosphorylate WT-Lnk (data not shown). We then evaluated the consequences of the loss of c-Src–mediated Lnk phosphorylation using CHO cells, which constitutively express human αIIbβ3 (29, 32) and were previously shown to spread on immobilized fibrino-

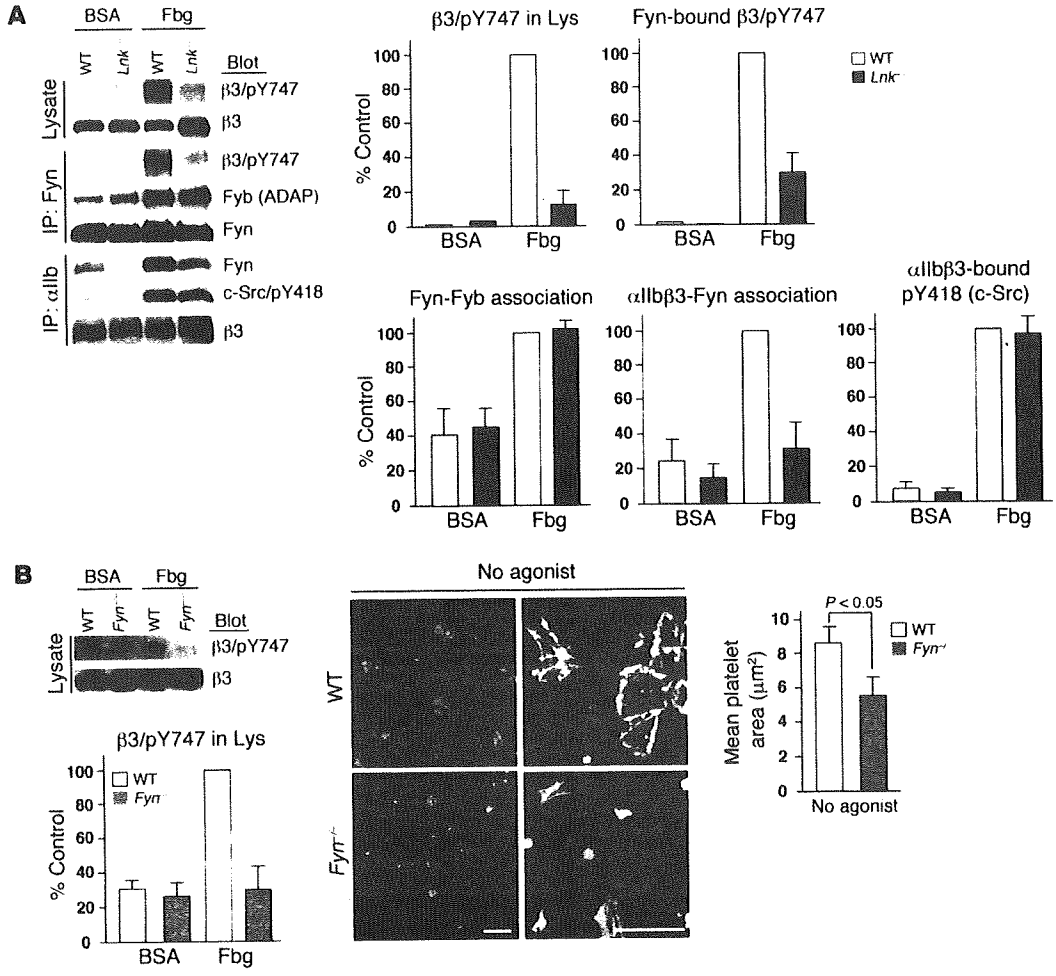

Figure 6

Lnk deficiency in platelets leads to reduced binding of Fyn to αIIbβ3 and reduced tyrosine phosphorylation of the cytoplasmic domain of the β3 integrin subunit. (**A**) WT and *Lnk*$^{-/-}$ platelets plated or maintained in suspension as in Figure 5A were lysed and analyzed by immunoblotting using anti–β3 integrin or anti–β3/p-Tyr747. In other sets, immunoprecipitation was elicited with anti-Fyn or anti-αIIb Ab. Each immunoblot panel is representative of 3 or 4 independent experiments, and estimated band densities are shown in the graphs. Band densities for WT samples from adherent platelets on fibrinogen were defined as 100%. Lys, lysates. (**B**) Washed platelets from WT and *Fyn*$^{-/-}$ mice were plated on fibrinogen for 45 minutes or maintained in suspension in a BSA-coated dish, lysed, and analyzed. The error bars in **A** and **B** indicate mean ± SD. (**C**) Left panels show the features of WT or *Fyn*$^{-/-}$ platelets allowed to spread on fibrinogen-coated coverslips for 45 minutes in the absence of agonist. The cells were fixed, permeabilized, and stained with Alexa 488 Fluor–phalloidin to visualize F-actin. Scale bars: 10 μm. The graph shows spreading quantified by computer analysis of their surface areas (mean ± SD).

gen in an Src kinase–dependent manner (32). When WT-Lnk or ΔC-Lnk was expressed as a GFP fusion protein, CHO cells expressing ΔC-Lnk showed fewer lamellipodia on fibrinogen than those expressing WT-Lnk (Supplemental Figure 5B). Thus, the absence of its C terminus again disrupted Lnk's ability to mediate formation of lamellipodia (Supplemental Figure 5B). Apparently, the C-terminal portion of Lnk and phosphorylation of Tyr536, which is likely regulated by c-Src, are key contributors to formation of lamellipodia and cell spreading mediated via integrin αIIbβ3.

Adherent Lnk$^{-/-}$ *platelets show reduced tyrosine phosphorylation of the β3 integrin subunit and reduced association of Fyn with αIIbβ3.* The importance of Src activation to outside-in αIIbβ3 signaling is well documented (4, 5, 31). Because Lnk appears to co-immunoprecipitate with both c-Src and Fyn (Figure 5B), we next asked whether Lnk might regulate the function of these kinases in platelets. During platelet aggregation or adhesion to fibrinogen, 2 conserved tyrosine residues in the β3 subunit, Tyr747 and Tyr759, are putatively targeted by Fyn, which is reportedly indispensable for clot retraction and prevention of re-bleeding from tail wounds (1, 8, 9). Moreover, Tyr747 is reportedly required for the binding of talin, filamin, c-Src, and other proteins essential for normal integrin signaling in platelets (33). We previously observed prominent phosphorylation of Tyr747 in WT platelets upon adherence to fibrinogen (10), but this response was severely impaired in *Lnk*$^{-/-}$ platelets (Figure 6A). Because it is likely that Fyn phosphorylates Tyr747 through direct interaction with the β3 cytoplasmic tail (9, 20, 31), we examined the extent to which Lnk deficiency affected (a) the association of Fyn with β3 and (b) the phosphorylation status of Tyr747 in plate-

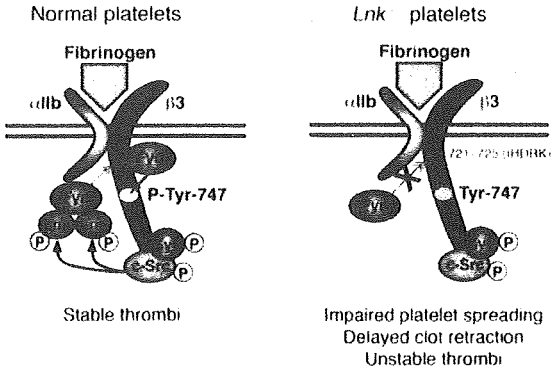

Figure 7
Model for outside-in signaling through αIIbβ3, c-Src, Fyn, and Lnk. Based on the present study, we propose that when activated, αIIbβ3 binds to fibrinogen, and a pool of c-Src constitutively bound to the cytoplasmic domain of the integrin β3 subunit initiates outside-in αIIbβ3 integrin signaling, which includes phosphorylation of Syk and its recruitment to αIIbβ3 independent of Lnk (5). The activated c-Src phosphorylates Tyr536 in a C-terminal portion of Lnk, where Lnk forms a dimeric or multimeric structure via the N-terminal domain (34). Lnk strongly facilitates Fyn recruitment to its binding site, residues 721–725 (IHDRK) in the β3 integrin tail, which may lead to phosphorylation of Tyr747 (P-Tyr747) within the β3 cytoplasmic domain of integrin αIIbβ3. Thereafter, phosphorylation of Tyr747 may facilitate thrombus stabilization in vitro and in vivo through a platelet contraction mechanism (7, 9, 40).

lets. We found that in WT platelets, Fyn co-immunoprecipitated with phosphorylated β3 and that this response was dependent upon fibrinogen ligation (Figure 6A, IP: Fyn). Furthermore, Fyn was bound to αIIbβ3 complexes immunoprecipitated 0 and 45 minutes after fibrinogen binding (Figure 6A, IP: αIIb, lanes BSA and Fbg, respectively), but this interaction was markedly diminished in *Lnk* platelets at the same time point. The association of Fyn with Fyb was augmented by fibrinogen binding independently of Lnk (Figure 6A, IP: Fyn), and the activation of c-Src bound to αIIbβ3 (assessed based on phosphorylation of Tyr418) was comparable (Figure 6A, IP: αIIb). That Fyn is constitutively associated with the β3 integrin subunit (20) suggests that Lnk contributes to the maintenance or strength of Fyn binding to the αIIbβ3-based signaling complex without affecting c-Src activation.

Finally, we assessed the effect of Fyn deficiency on tyrosine phosphorylation of the β3 subunit and the morphology of platelets spread on fibrinogen. *Fyn* platelets showed reduced phosphorylation of at least Tyr747 when bound to fibrinogen for 15 or 45 minutes (shown at 45 minutes, Figure 6B). In addition, in the absence of an agonist, *Fyn* platelets exhibited delayed and impaired spreading and somewhat reduced formation of lamellipodia on fibrinogen, even after 45 minutes (Figure 6C). *Fyn* platelets began spreading at about 20 minutes, by which time the spreading of WT platelets had already reached a plateau (data not shown). These results are consistent with the idea that Lnk sustains Fyn kinase activation of αIIbβ3, thereby regulating tyrosine phosphorylation of the β3 subunit.

Fyn-deficient mice exhibit a defect in thrombus formation similar to that seen in Lnk-deficient mice. To further examine the role of Fyn during thrombus formation in vivo, we assessed thrombus formation within mesenteric capillaries and arteries as we did for Lnk in the experiments shown in Figure 3, C and D. We found that *Fyn* mice exhibited impaired thrombus formation that was very similar to that seen in *Lnk* mice (Supplemental Figure 6 and Supplemental Videos 7 and 8). They also showed increased re-bleeding, but not prolonged initial bleeding times (data not shown), which is consistent with the results of Reddy et al. (20). Thus, Lnk and Fyn may act in concert to regulate αIIbβ3-based actin cytoskeletal reorganization leading to thrombus stabilization.

Discussion

Lnk is known to be a negative modulator of cytokine/growth factor receptor–mediated signaling (22) and to, perhaps, influence the motility of HSCs and progenitor cells, including their homing to (or lodging within) niches within the BM (16, 34). In addition, the proven importance of integrins and actin reorganization in HSC migration and homing (34, 35) and in megakaryocyte function (19) raises the possibility that Lnk modulates integrin signaling, but this idea has yet to be tested. In this report, we revealed a formerly unrecognized mechanism by which Lnk adaptor protein regulates integrin signaling in platelets and stabilizes developing thrombi in vivo. Using an in vivo $FeCl_3$-induced vessel occlusion model and direct imaging of platelet behavior, we showed that Lnk deficiency in platelets impairs stabilization of the developing thrombus under flow conditions, which may lead to an increase in re-bleeding events in *Lnk* (Figure 1C) and Lnk-chimeric (Supplemental Figure 2, right) mice. Through these mechanistic studies, we have been able to demonstrate that Lnk is required for platelets to fully spread on fibrinogen (Figure 4 and Supplemental Figure 3), for efficient fibrin clot retraction (Figure 4C), for platelet aggregation in the presence of lower concentrations of an agonist (Figure 4D), and for thrombus stability under flow conditions in vivo (Figures 2 and 3). Furthermore, the findings show that all of these effects of Lnk are mediated largely by αIIbβ3-dependent outside-in signaling, which is likely associated with tyrosine phosphorylation of the β3 integrin subunit (8) or Fyn tyrosine kinase (20). We also found that ligand binding to αIIbβ3 in platelets induces the formation of a protein complex that includes αIIbβ3, c-Src, Fyn, Fyb, and Lnk (Figure 5). Formation of this complex required Src kinase activity, which targeted the C-terminal portion of Lnk (Supplemental Figure 5). Finally, we showed that Lnk supports activation of Fyn within the αIIbβ3 complex, that Fyn in turn tyrosine phosphorylates the β3 subunit (Figure 6), and that the consequences of Lnk deficiency are mirrored by Fyn deficiency (Supplemental Figure 6). In contrast to the previously described constitutive association of c-Src or Fyn with β3 (4, 31), our results indicate that the efficient binding of Fyn, but not c-Src, to the αIIbβ3 complex requires the presence of Lnk (Figure 6). When situated in close proximity to αIIbβ3, Fyn may function as a positive regulator of β3 tyrosine phosphorylation (Figure 6B) (10, 28), which would contribute to the stabilization of the thrombus (Supplemental Figure 6) (9, 20), perhaps through association of Fyn with EphA4 (7) or Bcl-3 (36). Lnk thus appears to play a previously unappreciated role in facilitating integrin αIIbβ3 outside-in signaling by acting in concert with Fyn to phosphorylate the β3 subunit on Tyr747, thereby optimizing platelet cytoskeletal reorganization for stabilization of thrombi in vivo. We therefore conclude that Lnk may selectively promote Fyn kinase regulation of αIIbβ3 outside-in signaling in platelets.

One limitation of comparing thrombus formation in Lnk- and WT-chimeras is the need to compare platelets in mice of differ-

ent ages due to the higher capacity for megakaryopoiesis in *Lnk*$^{-/-}$ animals after BM transplantation. However, using intravital microscopy after laser-induced injury, we were able to compare thrombus formation in *Lnk*$^{-/-}$ and WT mice of the same age and show that thrombus formation is impaired in *Lnk*$^{-/-}$ animals despite higher numbers of circulating platelets (Figure 3, C and D). The reduced thrombus formation by Lnk-deficient platelets was even apparent 4 weeks after transplantation, at which time chimeric mice show slight thrombocytopenia, reflecting the fact that they are recovering from severe myelosuppression, and so are actively generating platelets. Furthermore, our in vitro study of the spreading of platelets from chimeric mice of different ages confirmed that the area of spread of platelets from Lnk-chimeras was consistently smaller than the area of spread of platelets from WT-chimeras. From these findings, we again conclude that Lnk deficiency leads to impaired platelet spreading independent of age or active megakaryopoiesis and contributes to the impaired stabilization of developing thrombi in vivo.

The small GTPase Rac1 and its guanosine exchange factor Vav contribute to the formation of lamellipodia during the adhesion of CHO-αIIbβ3 cells to fibrinogen (29, 37). The activation of Rac1 is mediated through 2 NxxY motifs (residues 744–747 and 756–759 in the β3 subunit) in the cytoplasmic tail of the β3 subunit (37). Reddy et al. recently demonstrated that CHO cells expressing a truncated form of αIIbβ3 lacking the distal NxxY motif (residues 756–759) fail to spread on fibrinogen, and the defect is rescued by overexpression of active Fyn (20). Those results indicate that Fyn activation may augment functions of the proximal NxxY motif (residues 744–747), presumably through phosphorylation of Tyr747 (8). Our results support that idea and indicate that Fyn, with the help of Lnk, is required for Tyr747 phosphorylation of β3 (Figure 6, A and B). In the model cell system, Lnk was directly tyrosine phosphorylated at Tyr536 by c-Src, which was required for formation of lamellipodia by CHO-αIIbβ3 cells immobilized on fibrinogen (Supplemental Figure 5). Because Lnk supports Fyn's association with the αIIbβ3 complex but is not required for c-Src activation or its association with the αIIbβ3 complex in platelets (Figure 6A), we propose the signaling cascade depicted in Figure 7. The Fyn binding region of β3 – residues 721–725 (IHDRK) (20) – is distinct from the c-Src binding region – residues 760–762 (RGT) (38). In normal platelets, the engagement of integrin αIIbβ3 initiates outside-in signaling through c-Src activation and Syk recruitment to the β3 tail (4, 5, 31), which is independent of Lnk. The activated c-Src presumably mediates tyrosine phosphorylation of Lnk, which leads to efficient recruitment/activation of Fyn at the β3 tail and phosphorylation of Tyr747 (Figure 7). We studied the effects of CVX on inside-out signaling by measuring fibrinogen binding to integrin αIIbβ3 and on outside-in signaling by studying platelet spreading on a collagen-coated surface (data not shown). The results so far indicate that Lnk is not involved in signaling mediated through GPVI, where Fyn also functions, and it appears that Lnk deficiency does not universally affect Fyn-coupled platelet receptors. Although the precise molecular mechanism is currently unknown, presumably the necessary machinery exists to ensure the specific and selective interaction of Lnk and the Fyn complex with the β3 integrin subunit.

It has been reported that the laser-induced injury model mainly reflects the tissue factor/thrombin–mediated pathway to platelet activation and is independent of the exposed collagen-GPVI and vWF-GPIbα interactions triggered by the loss of endothelium; conversely, $FeCl_3$-induced thrombus formation is collagen and vWF dependent (23, 25, 39). Nonetheless, it is reasonable to consider that our laser-induced injury model caused relatively mild damage to endothelial cells, as compared with previously reported experimental models (26). Consistent with that idea, we found that staining of the vasculature for *Griffonia simplicifolia* IB$_4$ isolectin showed the endothelial layer to be intact after laser-induced injury (Supplemental Figure 7). In addition, there was no extravasation of fluorescent dyes after laser injury, indicating that vascular permeability was unaffected by laser-induced injury (Supplemental Videos 1–8). Although, as with other methods, the precise mechanism and trigger of laser-induced thrombus formation remain unclear, it is unlikely that exposure of the extracellular matrix (mainly collagen) as a result of endothelial damage is a primary trigger. One alternative possibility is that thrombus formation is triggered by ROS, but ROS produced within the blood as a result of laser irradiation of hematoporphyrin and fluorescent dyes are readily washed away by the rapid blood flow. More likely, ROS produced within endothelial cells and/or stromal spaces are involved.

Given the mild damage to the endothelium and the lack of involvement of the collagen-GPVI and vWF-GPIbα interactions, the diminished thrombus formation seen in *Lnk*$^{-/-}$ platelets could reflect a defect in αIIbβ3-mediated signaling. Recently, 2 distinct phases in the stabilization of the primary hemostatic plug under flow conditions have been proposed. The first is a rapid phase linked to fibrin-independent platelet contractility (40), possibly accomplished through αIIbβ3-mediated outside-in signaling and the subsequent Rho kinase–dependent physical tightening of platelet-platelet adhesion contacts, for example, through ephrin/Eph kinases, JAM-A, or Sema4D (41). The second is a slower phase linked to thrombin generation and fibrin polymerization to stabilize the thrombus (40).

With our imaging system and laser-induced injury, we were able to observe the rapid phase of thrombus formation, which occurs within seconds, whereas $FeCl_3$-induced arterial occlusion occurs more than 20 minutes after injury. Using chimeric mice in which platelet counts were equalized, we observed that in vivo thrombus formation by *Lnk*$^{-/-}$ platelets was impaired in both models, although more significant deficiencies were detected in the laser-injury model (Figure 2C and Figure 3A).

Recent genome-wide association studies identified SNPs associated with type 1 diabetes and celiac disease, including a nonsynonymous SNP in exon 3 of LNK/SH2B3, encoding a pleckstrin homology domain (R262W) (42, 43). Notably, the same SNP was recently shown to be associated with increased eosinophil numbers and myocardial infarction (42, 43). Accordingly, it will be important to investigate the link between the sequence variation in LNK/SH2B3 and platelet function in patients.

In conclusion, we explored a new regulatory mechanism by which the adaptor protein Lnk contributes to the stabilization of developing thrombi. Lnk regulates integrin αIIbβ3–mediated signaling in platelets and is required for Fyn interaction with αIIbβ3 and efficient tyrosine phosphorylation of the β3 integrin subunit, leading to actin cytoskeletal reorganization. Because *Lnk*$^{-/-}$ mice do not exhibit spontaneous (or abnormal) bleeding or severe immune system dysfunction, we suggest that molecules that modulate outside-in signaling, including Lnk, might represent novel and safe therapeutic targets for the prevention of cardiovascular events. Such therapeutics would likely pose a smaller risk for bleeding than conventional drugs.

Methods

Cells, reagents, and mice. All reagents were from Sigma-Aldrich unless otherwise indicated. C57BL/6 mice congenic for the Ly5 locus (B6-Ly5.1) and *Lnk*$^{-/-}$ B6-Ly5.1 mice (22) were bred and maintained at the Animal Research Centers of the Institute of Medical Science, the University of Tokyo, and of the Research Institute, International Medical Center of Japan. *Lnk*$^{-/-}$ B6-Ly5.1 mice were first established on a C57BL/6 (B6-Ly5.2) background and backcrossed more than 12 times, after which they were crossed into the B6-Ly5.1 background. WT B6-Ly5.2 mice were purchased from Nihon SLC. *Fyn*$^{-/-}$ B6-Ly5.2 mice (44) were from T. Yamamoto (University of Tokyo). The protocol for this work was approved by the IACUCs of the Institute of Medical Science, University of Tokyo, and of the Research Institute, International Medical Center of Japan. The following Abs and reagents were used: anti-c-Src (327, a gift from J. Brugge, Harvard Medical School, Boston, Massachusetts, USA) (4, 31), anti-mouse αIIbβ3 (1B5, from B. Coller, Rockefeller University, New York, New York, USA), anti-human Lnk (from J. Hayashi, University of Maryland, Baltimore, Maryland, USA, or purchased from Abcam), anti-mouse Lnk (11), anti-Lcp2 and anti-Fyb (from G. Koretzky, University of Pennsylvania, Philadelphia, USA), anti-phospho-Src pY418 and anti-phospho-β3 pY773 (Y747 in mice) (Biosource International), anti-Syk (N-19), anti-Fyn (FYN3) and anti-β3 integrin (N-20) (Santa Cruz Biotechnology Inc.), anti-phosphotyrosine (4G10) and anti-Src (GD11) (Upstate Biochemical), anti-Fyb and anti-αIIb (MWReg30, BD Biosciences and Invitrogen). HRP-conjugated secondary Abs (Bio-Rad), Protein G Sepharose (GE Healthcare), protease inhibitor cocktail, aprotinin, and leupeptin (Roche Molecular Biochemicals), rhodamine-phalloidin, Alexa Fluor 488–conjugated fibrinogen, and Alexa Fluor 488–conjugated bovine IgG Abs (Molecular Probes, Invitrogen), purified human fibrinogen (American Diagnostica Inc), FITC-conjugated anti-mouse integrin α2, αIIb, and β3 and the FITC-Annexin-V kit (BD and Invitrogen), PE–anti-mouse GPIbα, FITC–anti-mouse GPVI, and PE–anti-mouse P-selectin (Emfret), and CVX (from T. Morita, Meiji Pharmaceutical University, Tokyo, Japan).

BM transplantation. BM from femurs was washed with PBS and counted. WT (10^7 per recipient mouse) or *Lnk*$^{-/-}$ (2×10^5 or 5×10^5) BM cells were intravenously transfused into 8-week-old male Ly-5.2 recipient mice. The recipients were then lethally irradiated at a dose of 9.5 Gy. Two, 4, 6, and 8 weeks later, PBLs were collected from the recipient mice, and chimerism was confirmed using a Ly5.1/Ly5.2 system.

Bleeding times. Tail bleeding assays were performed with 8- to 12-week-old *Lnk*$^{-/-}$ and WT male mice. Mice were anesthetized with 50 μg/ml pentobarbital, after which a 5-mm segment of the distal tip of the tail was cut off, and the tail was immediately immersed in PBS at 37°C. Tail bleeding times were defined as the time required for the bleeding to stop. Tail bleeding was monitored for at least an additional 60 seconds to detect possible re-bleeding (secondary bleeding), as previously described (8, 20, 45). We preliminarily confirmed that tail bleeding and re-bleeding times were comparable in B6-Ly5.1 and B6-Ly5.2 mice.

Measurement of $FeCl_3$-induced vessel occlusion times in carotid arteries. Mice were anesthetized by injection with urethane (1.5 g/kg), and a segment of the carotid artery was exposed. Thrombus formation was then triggered by applying 10% $FeCl_3$ solution to the adventitial side to induce endothelial cell injury (23). FITC-dextran solution (5 mg/kg BW, MW 150,000) was injected via the tail vein, and carotid blood flow was continuously monitored using fluorescence confocal microscopy to determine the time to occlusion.

Intravital microscopy and thrombus formation. To visually analyze thrombus formation in the microcirculation of the mesentery in living animals, we used in vivo laser injury and visualization techniques developed through modification of conventional methods (18, 24). Male mice were anesthetized by injection with urethane (1.5 g/kg), and a small incision was made so that the mesentery could be observed without being exteriorized. FITC-dextran (5 mg/kg BW) was injected into mice to visualize cell dynamics, while hematoporphyrin (1.8 mg/kg for capillary thrombi, 2.5 mg/kg for arterioles) was injected to produce ROS upon laser irradiation. Blood cell dynamics and production of thrombi were visualized during laser excitation (λ, 488 nm, 30 mW power). Sequential images were obtained for 20 seconds at 30 frames/s using a spinning-disk confocal microscope (CSU22, Yokogawa Electronics) and an EM-CCD camera (Impactron CCD; Nihon TI). The diameters of the examined capillaries were as follows: in Figure 3A, WT-chimera 6.56 ± 0.12 μm, Lnk-chimera 6.68 ± 0.06 μm (n = 30 vessels from 5 animals, P = 0.42); in Figure 3C, *Lnk*$^{-/-}$ 6.56 ± 0.12 μm, WT 6.46 ± 0.10 μm, *Lnk*$^{-/-}$ 6.56 ± 0.12 μm (n = 30 vessels from 5 animals, P = 0.26). In Figure 3D, diameters of the examined arterioles were as follows: WT 26.6 ± 4.5 μm, *Lnk*$^{-/-}$ 25.7 ± 3.4 μm (n = 10 vessels from 5 animals, P = 0.43). We also confirmed that thrombus formation within the vessels was comparable in the B6-Ly5.1 and B6-Ly5.2 mice.

Preparation of blood samples for analysis of platelet spreading and fibrinogen binding. For each experiment, blood samples were collected from 8–10 *Lnk*$^{-/-}$ and WT male mice (8–12 weeks old) by cardiac puncture after CO_2 treatment. Some collected samples were immediately transferred to plastic tubes containing one-sixth volume of acid-citrate-dextrose (ACD). Platelet-rich plasma (PRP) was obtained by centrifugation of whole blood at 150 *g* for 15 minutes without braking. To obtain the washed platelets used for most of the in vitro experiments, 1 μM PGE_1 and 2 U/ml apyrase were added, and the platelets were centrifuged at 750 *g* for 10 minutes. The sedimented platelets were then washed in modified Tyrode-HEPES buffer containing 1 μM PGE_1 plus 15% volume ACD and finally resuspended in an appropriate volume of Ca^{2+}-free modified Tyrode-HEPES buffer (10 mM HEPES [pH 7.4], 12 mM $NaHCO_3$, 138 mM NaCl, 5.5 mM glucose, 2.9 mM KCl, and 1 mM $MgCl_2$).

Confocal microscopic analysis of platelet spreading and immunoprecipitation assays. All confocal studies were performed using a Leica TCS SP2 microscope equipped with a 63×, 1.40 NA oil immersion objective (Leica), as described previously (46). Images were assembled using Adobe Photoshop. Analysis of platelet adhesion (cell number) and calculation of their surface area (spreading) were done using NIH ImageJ software (http://rsbweb.nih.gov/ij/).

The lysis buffer used for immunoprecipitation contained 2% Triton X-100 or 1% NP-40, 150 mM NaCl, 50 mM Tris-HCl (pH 7.4), 0.5 mM EGTA, 0.5 mM EDTA, 1 mM Na_3VO_4, 0.5 mM NaF, 0.5 mM PMSF, and 50 μg/ml leupeptin. Anti-αIIb was used for immunoprecipitation of αIIbβ3.

Flow cytometric measurement of fibrinogen-binding (activation of αIIbβ3) and P-selectin expression. Washed, rested platelets were incubated for 30 minutes at room temperature with 200 μg/ml Alexa Fluor 488–conjugated fibrinogen plus ADP, epinephrine, PAR4 agonist peptide, or PMA in a 50-μl final volume of modified Tyrode-HEPES buffer containing 0.2 mM $CaCl_2$. The binding of Alexa Flour 488–fibrinogen to platelets was quantified using an Aria flow cytometer (BD). Nonspecific binding was determined in the presence of 20 μg/ml 1B5. Specific binding was defined as total minus the nonspecific binding. P-selectin expression was measured similarly using a Canto-II flow cytometer (BD) with washed platelets in a 100-μl final volume (1×10^6 platelets).

Clot retraction assay. To obtain washed platelets, PRP from WT or *Lnk*$^{-/-}$ mice was diluted with 1 volume of modified Tyrode-HEPES buffer and centrifuged in the presence of 0.15 μM PGE_1. The sedimented platelets were then washed in modified Tyrode-HEPES buffer containing 0.15 μM PGE_1 and 1 mM EDTA and finally resuspended with modified Tyrode-HEPES buffer to adjust the number of platelets to 3×10^8/ml. Fibrin clot retraction was studied by incubating the clots in the presence of 2 U/ml

thrombin, 500 μg/ml fibrinogen, and 2 mM $CaCl_2$ for 1 or 2 hours at 37°C in an aggregometer cuvette as described previously (47, 48).

Plasmids and transfection of COS7 or CHO cells. COS7 and CHO-αIIbβ3 cells (provided by H. Kashiwagi, Osaka University, Osaka, Japan) were transfected using Lipofectamine 2000 methodology (Invitrogen). Constitutively active human c-Src mutant (Y530F)/pcDNA3 was obtained from T. Tezuka (University of Tokyo). Flag-tagged Lnk and the C-terminal deletion mutant (ΔC-Lnk) were constructed by PCR using previously constructed plasmids (34) as templates and reinserted into pcDNA3 vector. A Lnk cDNA cassette lacking the stop codon was generated by PCR and inserted into pcDNA-DEST47 (Invitrogen) to generate the expression vector for the Lnk-GFP fusion protein, as described previously (34).

Statistics. Differences between experimental and control animals were analyzed using 2-tailed Student's *t* tests. Incidence of re-bleeding times was evaluated by the χ^2 test. *P* values less than 0.05 were considered significant.

Acknowledgments

The authors thank J. Brugge, B. Coller, J. Hayashi, H. Kashiwagi, G. Koretzky, T. Morita, and T. Tezuka for providing reagents or cells and T. Yamamoto for *Fyn*-null mice. We are also grateful to J. Seita, H. Tsukui, A. Yamasaki, K. Wakabayashi, and M. Tajima for their excellent technical help. This work was supported by Grants-in-Aid and Special Coordination Funds for Promoting Science and Technology from the Ministry of Education, Culture, Sports, Science and Technology and from the Ministry of Health, Labour and Welfare, by the Japanese Sharyou Foundation (Tokyo, Japan), by the Uehara Memorial Foundation (Tokyo, Japan), and by the Mitsubishi Pharma Research Foundation (Osaka, Japan). H. Takizawa and S. Nishimura are supported by a fellowship for Japanese Junior Scientists from the Japan Society for the Promotion of Science.

Received for publication April 9, 2009, and accepted in revised form October 28, 2009.

Address correspondence to: Koji Eto, Division of Stem Cell Bank, The Institute of Medical Science, The University of Tokyo, 4-6-1 Shirokanedai, Minato-ku, Tokyo, 108-8639 Japan. Phone: 81-3-6409-2342; Fax: 81-3-6409-2343; E-mail: keto@ims.u-tokyo.ac.jp. Or to: Satoshi Takaki, Research Institute, International Medical Center of Japan, 1-21-1 Toyama, Shinjuku-ku, Tokyo, 162-8655 Japan. Phone: 81-3-3202-7181; Fax: 81-3-3208-5421; E-mail: stakaki@ri.imcj.go.jp.

1. Shattil SJ, Newman PJ. Integrins: dynamic scaffolds for adhesion and signaling in platelets. *Blood.* 2004;104(6):1606–1615.
2. Ruggeri ZM. Platelets in atherothrombosis. *Nat Med.* 2002;8(11):1227–1234.
3. Inoue O, et al. Laminin stimulates spreading of platelets through integrin alpha6beta1-dependent activation of GPVI. *Blood.* 2006;107(4):1405–1412.
4. Obergfell A, et al. Coordinate interactions of Csk, Src, and Syk kinases with [alpha]IIb[beta]3 initiate integrin signaling to the cytoskeleton. *J Cell Biol.* 2002;157(2):265–275.
5. Shattil SJ. Integrins and Src: dynamic duo of adhesion signaling. *Trends Cell Biol.* 2005;15(8):399–403.
6. Arias-Salgado EG, et al. PTP-1B is an essential positive regulator of platelet integrin signaling. *J Cell Biol.* 2005;170(5):837–845.
7. Prevost N, et al. Eph kinases and ephrins support thrombus growth and stability by regulating integrin outside-in signaling in platelets. *Proc Natl Acad Sci U S A.* 2005;102(28):9820–9825.
8. Law DA, et al. Integrin cytoplasmic tyrosine motif is required for outside-in alphaIIbbeta3 signalling and platelet function. *Nature.* 1999;401(6755):808–811.
9. Phillips DR, Nannizzi-Alaimo L, Prasad KS. Beta3 tyrosine phosphorylation in alphaIIbbeta3 (platelet membrane GP IIb-IIIa) outside-in integrin signaling. *Thromb Haemost.* 2001;86(1):246–258.
10. Xi X, et al. Tyrosine phosphorylation of the integrin beta 3 subunit regulates beta 3 cleavage by calpain. *J Biol Chem.* 2006;281(40):29426–29430.
11. Takaki S, et al. Control of B cell production by the adaptor protein lnk. Definition of a conserved family of signal-modulating proteins. *Immunity.* 2000;13(5):599–609.
12. Takaki S, Morita H, Tezuka Y, Takatsu K. Enhanced hematopoiesis by hematopoietic progenitor cells lacking intracellular adaptor protein, Lnk. *J Exp Med.* 2002;195(2):151–160.
13. Velazquez L, et al. Cytokine signaling and hematopoietic homeostasis are disrupted in Lnk-deficient mice. *J Exp Med.* 2002;195(12):1599–1611.
14. Tong W, Lodish HF. Lnk inhibits Tpo-mpl signaling and Tpo-mediated megakaryocytopoiesis. *J Exp Med.* 2004;200(5):569–580.
15. Tong W, Zhang J, Lodish HF. Lnk inhibits erythropoiesis and Epo-dependent JAK2 activation and downstream signaling pathways. *Blood.* 2005;105(12):4604–4612.
16. Buza-Vidas N, et al. Cytokines regulate postnatal hematopoietic stem cell expansion: opposing roles of thrombopoietin and LNK. *Genes Dev.* 2006;20(15):2018–2023.
17. Seita J, et al. Lnk negatively regulates self-renewal of hematopoietic stem cells by modifying thrombopoietin-mediated signal transduction. *Proc Natl Acad Sci U S A.* 2007;104(7):2349–2354.
18. Falati S, Gross P, Merrill-Skoloff G, Furie BC, Furie B. Real-time in vivo imaging of platelets, tissue factor and fibrin during arterial thrombus formation in the mouse. *Nat Med.* 2002;8(10):1175–1181.
19. Takizawa H, et al. Growth and maturation of megakaryocytes is regulated by Lnk/Sh2b3 adaptor protein through crosstalk between cytokine- and integrin-mediated signals. *Exp Hematol.* 2008;36(7):897–906.
20. Reddy KB, Smith DM, Plow EF. Analysis of Fyn function in hemostasis and alphaIIbbeta3-integrin signaling. *J Cell Sci.* 2008;121(Pt 10):1641–1648.
21. Fitau J, Boulday G, Coulon F, Quillard T, Charreau B. The adaptor molecule Lnk negatively regulates tumor necrosis factor-alpha dependent VCAM-1 expression in endothelial cells through inhibition of the ERK1 and -2 pathways. *J Biol Chem.* 2006;281(29):20148–20159.
22. Ema H, et al. Quantification of self-renewal capacity in single hematopoietic stem cells from normal and Lnk-deficient mice. *Dev Cell.* 2005;8(6):907–914.
23. Dubois C, Panicot-Dubois L, Merrill-Skoloff G, Furie B, Furie BC. Glycoprotein VI-dependent and -independent pathways of thrombus formation in vivo. *Blood.* 2006;107(10):3902–3906.
24. Nishimura S, et al. In vivo imaging in mice reveals local cell dynamics and inflammation in obese adipose tissue. *J Clin Invest.* 2008;118(2):710–721.
25. Dubois C, Panicot-Dubois L, Gainor JF, Furie BC, Furie B. Thrombin-initiated platelet activation in vivo is vWF independent during thrombus formation in a laser injury model. *J Clin Invest.* 2007;117(4):953–960.
26. Furie B, Furie BC. In vivo thrombus formation. *J Thromb Haemost.* 2007;5(Suppl 1):12–17.
27. Juliano RL, Redding P, Alahari S, Edin M, Howe A, Aplin A. Integrin regulation of cell signaling and motility. *Biochem Soc Trans.* 2004;32(Pt 3):443–446.
28. Blystone SD. Kinetic regulation of beta 3 integrin tyrosine phosphorylation. *J Biol Chem.* 2002;277(49):46886–46890.
29. Obergfell A, et al. The molecular adapter SLP-76 relays signals from platelet integrin alphaIIbbeta3 to the actin cytoskeleton. *J Biol Chem.* 2001;276(8):5916–5923.
30. Jordan MS, Singer AL, Koretzky GA. Adaptors as central mediators of signal transduction in immune cells. *Nat Immunol.* 2003;4(2):110–116.
31. Arias-Salgado EG, et al. Src kinase activation by direct interaction with the integrin beta cytoplasmic domain. *Proc Natl Acad Sci U S A.* 2003;100(23):13298–13302.
32. Salsmann A, Schaffner-Reckinger E, Kabile F, Plancon S, Kieffer N. A new functional role of the fibrinogen RGD motif as the molecular switch that selectively triggers integrin alphaIIbbeta3-dependent RhoA activation during cell spreading. *J Biol Chem.* 2005;280(39):33610–33619.
33. Petrich BG, et al. The antithrombotic potential of selective blockade of talin-dependent integrin alpha IIb beta 3 (platelet GPIIb-IIIa) activation. *J Clin Invest.* 2007;117(8):2250–2259.
34. Takizawa H, et al. Enhanced engraftment of hematopoietic stem progenitor cells by the transient inhibition of an adaptor protein, Lnk. *Blood.* 2006;107(7):2968–2975.
35. Cancelas JA, et al. Rac GTPases differentially integrate signals regulating hematopoietic stem cell localization. *Nat Med.* 2005;11(8):886–891.
36. Wevrich AS, et al. Signal-dependent translation of a regulatory protein, Bcl-3, in activated human platelets. *Proc Natl Acad Sci U S A.* 1998;95(10):5556–5561.
37. Berrier AL, Martinez R, Bokoch GM, LaFlamme SE. The integrin beta tail is required and sufficient to regulate adhesion signaling to Rac1. *J Cell Sci.* 2002;115(Pt 22):4285–4291.
38. Arias-Salgado EG, Lizano S, Shattil SJ, Ginsberg MH. Specification of the direction of adhesive signaling by the integrin beta cytoplasmic domain. *J Biol Chem.* 2005;280(33):29699–29707.
39. Izuhara Y, et al. Inhibition of plasminogen activator inhibitor-1: its mechanism and effectiveness on coagulation and fibrosis. *Arterioscler Thromb Vasc Biol.* 2008;28(4):672–677.
40. Ono A, et al. Identification of a fibrin-independent platelet contractile mechanism regulating primary hemostasis and thrombus growth. *Blood.* 2008;112(1):90–99.
41. Brass LF, Zhu L, Stalker TJ. Novel therapeutic targets at the platelet vascular interface. *Arterioscler Thromb Vasc Biol.* 2008;28(3):s43–s50.
42. Hunt KA, et al. Newly identified genetic risk vari-

ants for celiac disease related to the immune response. *Nat Genet.* 2008;40(4):395–402.
43. Gudbjartsson DF, et al. Sequence variants affecting eosinophil numbers associate with asthma and myocardial infarction. *Nat Genet.* 2009;41(3):342–347.
44. Yagi T, et al. Regional localization of Fyn in adult brain: studies with mice in which fyn gene was replaced by lacZ. *Oncogene.* 1993;8(12):3343–3351.
45. Kasirer-Friede A, et al. ADAP is required for normal alphaIIbbeta3 activation by VWF/GP Ib-IX-V and other agonists. *Blood.* 2007;109(3):1018–1025.
46. Eto K, et al. The WAVE2/Abi1 complex differentially regulates megakaryocyte development and spreading: implications for platelet biogenesis and spreading machinery. *Blood.* 2007;110(10):3637–3647.
47. Prevost N, Kato H, Bodin L, Shattil SJ. Platelet integrin adhesive functions and signaling. *Methods Enzymol.* 2007;426:103–115.
48. Suzuki-Inoue K, et al. Involvement of Src kinases and PLCgamma2 in clot retraction. *Thromb Res.* 2007;120(2):251–258.

balt3/zbc-bc/zbc-bc/zbc04409/zbc9087-09z | xppws S=1 | 21/8/09 8:31 | 4/Color Figure(s) F2,4 | ARTNO: M109.038802

THE JOURNAL OF BIOLOGICAL CHEMISTRY VOL. 284, NO. ??, pp. 1–xxx, ???? ??, 2009

Molecular Basis for E-cadherin Recognition by Killer Cell Lectin-like Receptor G1 (KLRG1)*[S]

Received for publication, June 29, 2009, and in revised form, July 30, 2009. Published, JBC Papers in Press, August 4, 2009, DOI 10.1074/jbc.M109.038802

Seiko Nakamura[‡], Kimiko Kuroki[‡], Izuru Ohki[‡], Kaori Sasaki[‡], Mizuho Kazikawa[‡], Takuma Maruyama[§], Masayuki Ito[§1], Yosuke Kameda[§], Mitsuhiko Ikura[¶], Kazuo Yamamoto[§], Naoki Matsumoto[§], and Katsumi Maenaka[‡2]

From the [‡]Medical Institute of Bioregulation, Kyushu University, 3-1-1 Maidashi, Higashi-ku, Fukuoka, Fukuoka 812-8582, Japan, the [§]Department of Integrated Biosciences, Graduate School of Frontier Sciences, University of Tokyo, Kashiwa, Chiba 277-8562, Japan, and the [¶]Division of Signaling Biology, Ontario Cancer Institute and Department of Medical Biophysics, University of Toronto, Toronto, Ontario M5G 2M9, Canada

The killer cell lectin-like receptor G1, KLRG1, is a cell surface receptor expressed on subsets of natural killer (NK) cells and T cells. KLRG1 was recently found to recognize E-cadherin and thus inhibit immune responses by regulating the effector function and the developmental processes of NK and T cells. E-cadherin is expressed on epithelial cells and exhibits Ca^{2+}-dependent homophilic interactions that contribute to cell-cell junctions. However, the mechanism underlying the molecular recognition of KLRG1 by E-cadherin remains unclear. Here, we report structural, binding, and functional analyses of this interaction using multiple methods. Surface plasmon resonance demonstrated that KLRG1 binds the E-cadherin N-terminal domains 1 and 2 with low affinity (K_d ~7–12 μM), typical of cell-cell recognition receptors. NMR binding studies showed that only a limited N-terminal region of E-cadherin, comprising the homodimer interface, exhibited spectrum perturbation upon KLRG1 complex formation. It was confirmed by binding studies using a series of E-cadherin mutants. Furthermore, killing assays using KLRG1$^+$NK cells and reporter cell assays demonstrated the functional significance of the N-terminal region of E-cadherin. These results suggest that KLRG1 recognizes the N-terminal homodimeric interface of domain 1 of E-cadherin and binds only the monomeric form of E-cadherin to inhibit the immune response. This raises the possibility that KLRG1 detects monomeric E-cadherin at exposed cell surfaces to control the activation threshold of NK and T cells.

AQ: A

Fn3 Natural killer (NK)[3] cells play a critical role in the innate immune system because of their ability to kill other cells. For example, NK cells can kill virus-infected cells and tumor cells without presensitization to a specific antigen, and they produce various cytokines, including interferon-γ and tumor necrosis factor-α (1). NK cells are controlled by both inhibitory and activating receptors that are expressed on their surfaces (2). The killer cell Ig-like receptor, Ly49, CD94/NKG2, and paired Ig-like type 2 receptor families include both inhibitory and activating members and thus are designated as paired receptor families. On the other hand, some inhibitory receptors, including KLRG1 (killer cell lectin-like receptor G1), and activating receptors, such as NKG2D, also exist. The integration of the signals from these receptors determines the final functional outcome of NK cells.

AQ: B

These inhibitory and activating receptors can also be divided into two structurally different groups, the Ig-like receptors and the C-type lectin-like receptors, based on the structural aspects of their extracellular regions. The Ig-like receptors include killer cell Ig-like receptors and the leukocyte Ig-like receptors, and the C-type lectin-like receptors include CD94/NKG2(KLRD/KLRC), Ly49(KLRA), NKG2D(KLRK), NKR-P1(KLRB), and KLRG1. Many of these immune receptors recognize major histocompatibility complex class I molecules or their relatives (2–4), but there are still many orphan receptors expressed on NK cells. KLRG1 was one such orphan receptor; however, E-cadherin was recently found to be a ligand of KLRG1 (5, 6). Although major histocompatibility complex-receptor interactions have been extensively examined, the molecular basis of non-major histocompatibility complex ligand-receptor recognition is poorly understood.

KLRG1 is a type II membrane protein, with one C-type lectin domain in the extracellular region, one transmembrane region, and one immunoreceptor tyrosine-based inhibitory motif. KLRG1 is expressed on a subset of mature NK cells in spleen, lungs, and peripheral blood during normal development. KLRG1 expression is induced on the surface of NK cells during viral responses (7, 8). NK cells expressing KLRG1 produce low levels of interferon-γ and cytokines and have a slow *in vivo* turnover rate and low proliferative responsiveness to interleukin-15 (9). Furthermore, KLRG1 is recognized as a marker of some T cell subsets, as follows. KLRG1 defines a subset of T cells, short lived effector CD8 T cells (SLECs), which are mature effector cells that express high levels of KLRG1 and cannot be differentiated into long lived memory CD8 T cells. In addition, memory precursor

* This work was supported in part by the Ministry of Education, Culture, Sports, Science and Technology, and the Japan Bio-oriented Technology Research Advancement Institute (BRAIN).

ZSI [S] The on-line version of this article (available at http://www.jbc.org) contains supplemental Table S1 and Figs. S1–S3.

[1] Supported by the Canadian Cancer Society/National Cancer Institute of Canada and the Canadian Research Chair program.

[2] To whom correspondence should be addressed: Medical Institute of Bioregulation, Kyushu University, 3-1-1 Maidashi, Higashi-ku, Fukuoka, Fukuoka 812-8582, Japan. Tel.: 81-92-642-6998; Fax: 81-92-642-6998; E-mail: kmaenaka-umin@umin.net.

[3] The abbreviations used are: NK, natural killer; SLEC, short lived effector CD8 T cell; MES, 4-morpholineethanesulfonic acid; SPR, surface plasmon resonance; AUC, analytical ultracentrifugation; HSQC, heteronuclear sequential quantum correlation; PE, phycoerythrin.

effector cells express low levels of KLRG1 and harbor the potential to become long lived memory CD8 T cells (10). Since SLECs exhibit stronger effector function than memory precursor effector cells, it is potentially beneficial, in terms of preventing harmful excess cytotoxicity, that SLECs express KLRG1 at a higher level to inhibit the immune response. Taken together, the expression of KLRG1 during the viral response and normal development might confer the inhibition of effector function and the regulation of NK and T cell proliferation (9).

E-cadherin plays a pivotal role in Ca^{2+}-dependent cell-cell adhesion and also contributes to tissue organization and development (11–14). E-cadherin is primarily expressed on epithelial cells, and its extracellular region consists of several domains that include cadherin motifs (15, 16). These domains mediate Ca^{2+}-dependent homophilic interactions to facilitate cell adhesion. When E-cadherins form cis- or trans-homodimers, they utilize their N-terminal regions as an interface, which can dock with domain 1 of another E-cadherin to form strand exchange (17). Therefore, the N-terminal region plays important roles in homophilic binding and cell adhesion.

KLRG1 recognizes E-cadherins (and other class I cadherins), which are widely expressed in tissues and form tight adhesive cell-cell junctions, and Ito *et al.* (5) demonstrated that E-cadherin binding by KLRG1 inhibits NK cytotoxicity. Further, Gründermann *et al.* (6) showed that the E-cadherin-KLRG1 interaction inhibits the antigen-induced proliferation and induction of the cytolytic activity of CD8 T cells. Therefore, it is plausible that E-cadherin recognition by KLRG1, expressed on the surfaces of NK cells and T cells, may raise their activation thresholds by transducing inhibitory signals. Such an inhibition would prevent the excess injury of normal cells, which might result in inflammatory autoimmune diseases. KLRG1 may also have an important role in monitoring and removing cancer cells that lose E-cadherin expression. A recent report demonstrated that N-terminal domains 1 and 2 of E-cadherin are critical for KLRG1 recognition (18); however, despite accumulating evidence supporting the functional importance of the E-cadherin-KLRG1 interaction, the molecular basis of this interaction is poorly understood. Here, we report that the N-terminal region of E-cadherin, comprising the dimer interface, is the binding site for KLRG1. This suggests that KLRG1 does not recognize the dimeric form of E-cadherin but rather recognizes the monomeric form, which is exposed on the cell surfaces of disrupted or infected cells. This may suppress excess immune responses.

EXPERIMENTAL PROCEDURES

Preparation of Recombinant Proteins—The plasmid pET15bEC-D1D2(His10Xa), encoding domains 1 and 2 of E-cadherin, with a His_{10} tag, a spacer sequence, and a Factor Xa recognition site at the N terminus (EC-D1D2(His10Xa)), and pET15bEC-D2D3(His6) encoding domains 2 and 3 (residues 109–332) with an additional His_6 tag (EC-D2D3(His6)) were used to express recombinant proteins in *Escherichia coli* strain BL21 (DE3) pLysS. Soluble EC-D1D2(His10Xa) was subjected to Ni^{2+}-nitrilotriacetic acid affinity chromatography (HisTrapFF, 5 ml; GE Healthcare), or the inclusion bodies of EC-D1D2(His10Xa) were dissolved in guanidine buffer (6 M guanidine HCl, 50 mM MES-NaOH, pH 6.5, 100 mM NaCl, 10 mM EDTA). To refold the recombinant protein, 10–20 mg of solubilized inclusion bodies were gradually diluted by the addition of refolding buffer (20 mM Tris-HCl, pH 7.9, 300 mM NaCl, 10% glycerol, 1 mM phenylmethylsulfonyl fluoride) at 4 °C, into a final volume of 1 liter. The resulting solution was stirred for 2 days and was concentrated to 5–10 ml by a VIVA FLOW system and an Amicon Ultra filter (Millipore). The protein was purified by gel filtration chromatography (HiLoad26/60 Superdex 75 pg; GE Healthcare). After purification, EC-D1D2(His10Xa) was treated with Factor Xa to cleave the extra amino acids. The resulting EC-D1D2 protein was designated as EC-D1D2. EC-D2D3(His6) was prepared by the same method as the refolded EC-D1D2. AQ: C

The DNA encoding the extracellular region (residues 72–188) of *Mus musculus* KLRG1 was ligated into pET3c, to create the plasmid pET3cKLRG1. The recombinant protein was expressed as inclusion bodies and was refolded, in a similar manner as EC-D1D2 and EC-D2D3. The refolded protein was purified by gel filtration chromatography (Fig. 1). For surface plasmon resonance (SPR) analysis, a biotinylated version of KLRG1 was prepared, as described previously (5).

SPR—Recombinant cadherins, including the Ala-scanning mutants, were dissolved in HBS-P buffer (10 mM HEPES, pH 7.4, 150 mM NaCl, 0.005% Surfactant P20) (BIAcore AB). SPR experiments were performed with a BIAcore2000 (Biacore AB). Biotinylated KLRG1 was immobilized on the CM5 sensor chip (BIAcore AB), onto which streptavidin had been covalently coupled. Biotinylated bovine serum albumin was used as a negative control protein. All cadherin samples were injected over the immobilized KLRG1 protein, at a flow rate of 10 μl/min, in HBS-P buffer with 10 mM $CaCl_2$ or 3 mM EDTA (for the Ca^{2+}-free conditions, as indicated throughout). The binding response at each AQ: D concentration was calculated by subtracting the equilibrium response measured in the control flow cell from the response in each sample flow cell. The data were analyzed using the BIA evaluation version 4.1 (Biacore AB) and ORIGIN version 7 software (Microcal Inc.). Affinity constants (K_d) were derived by nonlinear curve fitting of the standard Langmuir binding isotherm.

Analytical Ultracentrifugation (AUC)—AUC was carried out using a Beckman Optima XL-I analytical ultracentrifuge with absorption optics, an An-50 Ti rotor, and standard double-sector centerpiece cells. Sedimentation equilibrium measurements were performed at 4 °C, and concentration profiles were recorded at 0, 20, 3, 3, and 3 h after the velocity of the rotor AQ: E reached 9,000, 14,000, and 20,000 rpm. At each time and velocity, one scan was collected. Data were analyzed using the standard Optima XL-I data analysis software. All of the protein samples were in 20 mM Tris-Cl buffer, pH 7.4, with 100 mM NaCl. Monomeric EC-D1D2 and monomeric KLRG1 were mixed at a molar ratio of 1:1 without calcium.

NMR Analysis of E-cadherin Binding to KLRG1—Uniformly ^{15}N-labeled EC-D1D2 was expressed in *E. coli* BL21(DE3) pLysS bearing the plasmid pET15bEC-D1D2(His10Xa), grown in M9 minimal medium containing 1 g/liter $^{15}NH_4Cl$, and was prepared by the same method used for the unlabeled EC-D1D2. KLRG1 was prepared as described previously. The KLRG1 and EC-D1D2 proteins were both dissolved in the HBS-E buffer (10 mM HEPES, pH 7.4, 150 mM NaCl, 3 mM EDTA). For the direct